frontiers | Frontiers in Energy Research

TYPE Original Research
PUBLISHED 18 January 2024
DOI 10.3389/fenrg.2023.1342085

OPEN ACCESS

EDITED BY
Kumaran Kadirgama,
Universiti Malaysia Pahang, Malaysia

REVIEWED BY
Nima Khosravi,
Other, Iran
Mohamed Salem,
University of Science Malaysia (USM), Malaysia

*CORRESPONDENCE
Shitharth Selvarajan,
s.selvarajan@leedsbeckett.ac.uk

RECEIVED 21 November 2023
ACCEPTED 31 December 2023
PUBLISHED 18 January 2024

CITATION
Srilakshmi K, Gaddameedhi S, Borra SR, Balachandran PK, Reddy GP, Palanivelu A and Selvarajan S (2024), Optimal design of solar/wind/battery and EV fed UPQC for power quality and power flow management using enhanced most valuable player algorithm. *Front. Energy Res.* 11:1342085. doi: 10.3389/fenrg.2023.1342085

Optimal design of solar/wind/battery and EV fed UPQC for power quality and power flow management using enhanced most valuable player algorithm

Koganti Srilakshmi[1], Sravanthy Gaddameedhi[1], Subba Reddy Borra[2], Praveen Kumar Balachandran[3], Ganesh Prasad Reddy[4], Aravindhababu Palanivelu[5] and Shitharth Selvarajan[6]*

[1]Department of Electrical and Electronics Engineering, Sreenidhi Institute of Science and Technology, Hyderabad, India, [2]Department of Information Technology, Malla Reddy Engineering College for Women, Hyderabad, India, [3]Department of Electrical and Electronics Engineering, Vardhaman College of Engineering, Hyderabad, India, [4]Department of Electrical and Electronics Engineering, A.M Reddy Memeorial College of Engineering, Guntur, AP, India, [5]Department of Electrical Engineering, Annamalai University, Chidambaram, TN, India, [6]Cyber Security and Digital Forensics, School of Built Environment, Engineering and Computing, Leeds Beckett University, Leeds, United Kingdom

The behavior and performance of distribution systems have been significantly impacted by the presence of solar and wind based renewable energy sources (RES) and battery energy storage systems (BESS) based electric vehicle (EV) charging stations. This work designs the Unified Power Quality Conditioner (UPQC) through optimal selection of the active filter and PID Controller (PIDC) parameters using the enhanced most valuable player algorithm (EMVPA). The prime objective is to effectively address the power quality (PQ) challenges such as voltage distortions and total harmonic distortions (THD) of a distribution system integrated with UPQC, solar, wind, BESS and EV (U-SWBEV). The study also aims to manage the power flow between the RES, grid, EV, BESS, and consumer loads by artificial neuro-fuzzy interface system (ANFIS). Besides, this integration helps to have a reliable supply of electricity, efficient utilization of generated power, and effective fulfillment of the demand. The proposed scheme results in a THD of 4.5%, 2.26%, 4.09% and 3.98% for selected four distinct case studies with power factor to almost unity with an appropriate power sharing. Therefore, the study and results indicate that the ANFIS based power flow management with optimal design of UPQC addresses the PQ challenges and achieves the appropriate and effective sharing of power.

KEYWORDS

power flow management, artificial neuro-fuzzy interface system, enhanced most valuable player algorithm, total harmonic distortion, power quality

1 Introduction

The integration of RES into the distribution network has gained more attention in the past few decades for lessening the burden on VSC's and reducing the necessity of higher device ratings. A novel solar-integrated UPQC configuration has been developed to effectively address the PQ problems. The various difficulties in exploiting renewable energy sources (RES) and various approaches for overcoming these difficulties have been discussed in (Madurai Elavarasan et al., 2020a; Madurai Elavarasan et al., 2020b; Elavarasan, 2020). Due to the intrinsic unpredictability of solar PV (SPV) systems, the grid is subjected to harmonic distortions, thereby affecting grid voltages and currents. FACTS devices have thus been used to reduce total harmonic distortions (THD) besides handling voltage stability-related issues and enhancing PQ of the grid (Shafiullah et al., 2018; Ashok Kumar and Indragandhi, 2020; Mohamed, 2020).

The benefits in view of enhancing PQ of UPQC in grid-connected SPV systems were investigated (Paramanik et al., 2019). A thorough analysis was focused on the features, charging methods, and benefits of electric vehicles (EVs) (Kong and Karagiannidis, 2016; Chellaswamy and Ramesh, 2017; Nunes and Brito, 2017). The UPQC was exhibited to be superior than those of DSTATCOM and DVR in terms of multitasking abilities, and employed with intended goals of raising power factor (PF), decreasing THD, boosting profiles of voltage, and boosting PQ of the system (Amirullah et al., 2020). The FLC was applied for integration of battery energy storage systems (BESS) with EVs for realizing better PQ, increased overall reliability of the grid with RES (Vivas et al., 2020).

The firefly optimization method, which simulates predator-prey dynamics, was employed to optimize the design of shunt active power filters for reducing the THD and enhancing the PF (Mahaboob et al., 2019). A PI-controller fine-tuning for SHAPF was devised using an Ant Colony Algorithm to minimize THD across various load combinations (Sakthivel et al., 2015). A novel control system incorporating both fuzzy logic and back-propagation was introduced for optimizing THD and enhancing PF in the context of a 5-level UPQC (Nagireddy et al., 2018). Nevertheless, in the micro-grid associated distribution system, PQ issues were resolved by employing UPQC to handle current and voltage imperfections. An adaptive network-based fuzzy inference system was introduced to enhance system efficiency and utilization (Renduchintala et al., 2021). A hybrid control technique that combines the Improved Bat Algorithm and Moth Flame Algorithm optimization was created to tackle PQ concerns within a micro-grid system, to minimize the error function related to power fluctuations. Furthermore, the operational costs of RESs were reduced by optimally tuning the K_p and K_i parameters (Rajesh et al., 2021).

Furthermore, a novel hybrid approach through integration of Enhanced Efficient Global Optimization with ANN techniques was introduced for shunt active power filter (SHAPF). This approach was designed to diminish current signal distortions and enhance the quality of power delivery in the distribution network (Ganesan and Srinath, 2019). Moreover, an examination of the power flow analysis of the UPQC was conducted on a three-phase distribution system under different operating conditions, focusing on the impedance matching technique (Zhao et al., 2021). A method utilizing self-tuning filters was devised for UPQC in conjunction with renewable energy sources to tackle PQ concerns (Mansoor et al., 2020). Concurrently, an implementation of ANN was applied to the Solar PV-powered UPQC to mitigate grid current THD during voltage variations such as sag and swell. Additionally, the effectiveness of this approach was assessed through a comparison with the State Repetitive Control and reactive power theory methods across diverse load scenarios (Okwako et al., 2022). However, to minimize system THD, a unique modified UPQC has been developed with multiple goals and variables that be optimized by employing the BHO and PSO approaches to change the PIC variables (Khosravi et al., 2023). In addition, a proposal was made to link AC/DC microgrid to the grid using power-compensating techniques to reduce the amplitudes of harmonics. This involves optimizing the coefficients of gain in certain filter compensation devices. The optimized coefficients were associated with a PIC including the cost functions incorporated the controller's error, current harmonics, and voltage harmonics (Khosravi et al., 2021).

The optimization of the gain coefficients for the MAPF and PFCK controllers was carried out hierarchically using the Harris hawk optimization, ABC, grasshopper optimization algorithm, and DE. This optimization was applied to the three control loops, which include voltage and current harmonics, as well as the system controller error. The goal was to reduce the range of these harmonics to within acceptable limits (Khosravi et al., 2022). A novel THD compensation scheme was developed for a hybrid micro-grid, employing a filter compensation device. The primary objective of this system is to mitigate the magnitude of the voltage and current harmonics (Khosravi Nima et al., 2021).

An extensive investigation was conducted to offer valuable insights into the influence of FACTS deployment on the integration of energy from renewable sources and the reduction of carbon emissions. The study examines the impact of many factors on sustainable energy entry, including system loading patterns, the placement of renewable power, and the placement of FACTS (Omid Mirzapour et al., 2023). Subsequently, a technique for reducing a lumped parameter thermal model was proposed, utilizing sensitivity analysis. This method aims to streamline the thermal model while still preserving the appropriate level of accuracy. The results demonstrated minimal discrepancy between the simplified thermal model approximation and the entire model, as evidenced by the low error (Mirzapour et al., 2018). The ANFIS model was created based on 390 metrics founded in literature (Seyed Alizadeh et al., 2021). However, vehicles powered by fossil fuels have been identified as the primary contributor to air pollution in urban areas, despite the advantages of electric automobiles in large cities. Additionally, they pose technical difficulties for electric electrical distribution systems (Pazouki and Olamaei, 2019). Besides, a mathematical model for efficiently scheduling and organizing the energy points in smart homes was designed to consider the demand of the smart home energy hub and classifies it into distinct types of loads. In

10.3389/fenrg.2023.1342085

TABLE 1 Literature survey.

Ref	PQ problems					Power flow management	Loads			EV	Optimization
[No]	Control	THD	DC link stabilization	Swell & sag	Voltage harmonics		Active power	Rectifier bridge	Unbalanced		Algorithm
Amirullah et al. (2020)	Fuzzy	*	*	*		*	*				
Vivas et al. (2020)	Fuzzy					*	*				
Mahaboob et al. (2019)	PI	*	*					*	*		*
Sakthivel et al. (2015)	PI	*						*	*		*
Nagireddy et al. (2018)	Neuro-Fuzzy	*		*				*			
Renduchintala et al. (2021)	Neuro-Fuzzy	*		*				*			
Rajesh et al. (2021)	PI	*	*					*			
Ganesan and Srinath (2019)	Fractional order PID	*						*	*		*
Zhao et al. (2021)	PI	*									
Mansoor et al. (2020)	Neural Network	*	*	*	*			*	*		
Okwako et al. (2022)	Neural Network	*	*	*				*	*		
U-WBEV	**EMVPA-PIDC**	*	*	*	*	*	*	*	*	*	*

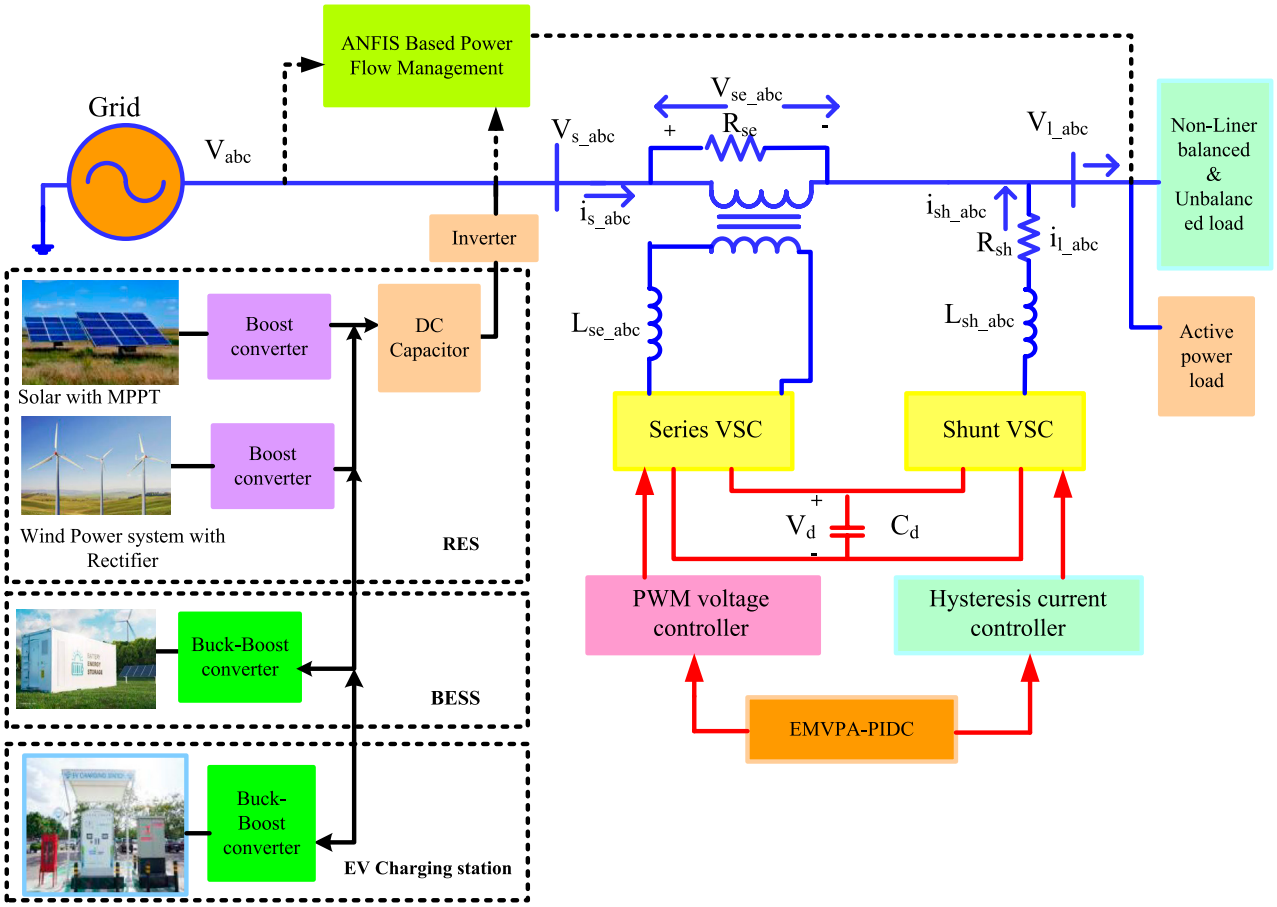

FIGURE 1
Structure of U-SWBEV.

TABLE 2 PV, wind, BESS and EV ratings.

Device	Configuration	Values
PV single panel (Sun power SPR-215-WHT-U)	PV cells connected in parallel, series	45, 10
	Rated Power	228.735 W
	SOC	8.18A
	OCV	37.1 V
	Under $P_{max}V_{PV}$&I_{PV}	29.9V/7.65A
Li-ion battery	Fully charge voltage	326.6 V
	Rated Q	400 A h
	COV	225 V
	NOV	300 V
	SOCB	95%
Wind Turbine	Nominal turbine P_{mop}	30 kW
	Maximum Θ_p	45deg
	Base V_W	15 m/s
	Maximum rate of change of Θ_p	25deg./second

TABLE 3 Lower and upper bonds for decision variables.

Decision variable	K_p	K_i	K_d	R_{se}	R_{sh}	L_{se}	L_{sh}
Lower	0.0001	0.0001	0.001	0	0	0.01	0.01
Upper	100	100	100	10	0.5	10	10

TABLE 4 Grid and load values chosen.

Source grid	V_S: 415V; f: 50 Hz
DC link capacitor	V_{dc}: 470V; C_{dc}: 100 μF
Loads	1. Rectifier bridge load R = 60; L = 0.15e-3
	2. Active power load: P_{L1} = 6 kW
	3. Rectifier bridge load R = 30; L = 20e-3
	4. Unbalanced load R1 = 10, R2 = 40, R3 = 70; L1 = 0.05 e−3, L2 = 0.1e-3, L3 = 0.15e-3
	5. Active and reactive power load R = 4kW; L = 1000Vars

TABLE 5 Test cases.

Condition	Case1	Case2	Case3	Case4
Fixed solar irradiation	*		*	
Varying solar irradiation		*		*
15 m/s wind velocity	*			*
11 m/s wind velocity		*	*	
Disturbance	*			
Swell		*		
Sag				*
Flicker			*	
Load 1	*		*	*
Load 2			*	*
Load 3		*		
Load 4			*	
Load 5	*	*		

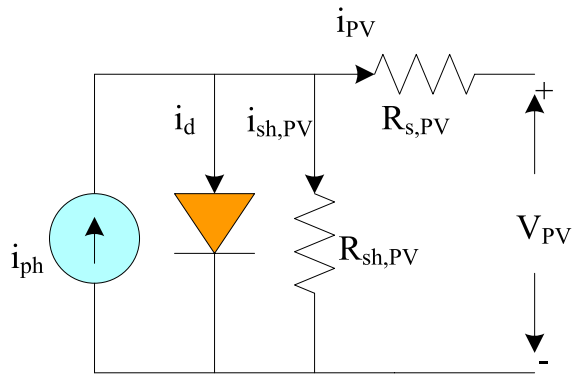

FIGURE 2
Single diode PV cell model.

addition, it encompasses the requirements for heating, cooling, and water, as stated in reference (Pazouki and Haghifam, 2021).

The development of the most valuable player algorithm involved the removal of undesirable and offensive players in order to avoid inefficient strategies and achieve rapid convergence. Subsequently, a new solution approach incorporating the improved most valuable player algorithm is proposed for addressing the optimal power flow problem. (Srilakshmia et al., 2020). On the other hand, optimized AI based techniques were adapted to renewable energy sources associated UPQC address PQ issues (Srilakshmi et al., 2022a; Srilakshmi et al., 2022b; Srilakshmi et al., 2023a; Srilakshmi et al., 2023b; Ramadevi et al., 2023).

As listed in Table 1, it is evident from the existing literature that the most recent research articles have predominantly concentrated on the application of UPQC in conjunction with RES, such as SPV and WSS. These studies have explored distinct control methods to enhance PQ by including BESS. However, there has been neglected the power flow management by the incorporation of EVs into these systems along with the optimal selection of controller and filter parameters of UPQC using metaheauristic algorithms.

It is worth noting that, particularly during periods of peak demand on the grid, excessive demand for power can be effectively managed using both BESS and EVs. This dual approach not only improves PQ but also facilitates power flow management concurrently. The key contributions of this study are outlined as follows:

- Development of an ANFIS-based hybrid control system to manage the power flow among the EVs, BESS, WES, RES and the grid.
- Optimal tuning of gain parameters of PIDC for shunt converter in addition to the selection of shunt and series filter parameters of UPQC by using EMVPA.
- Lowering the THD in the source side current and load terminal voltage, and mitigating grid voltage-related

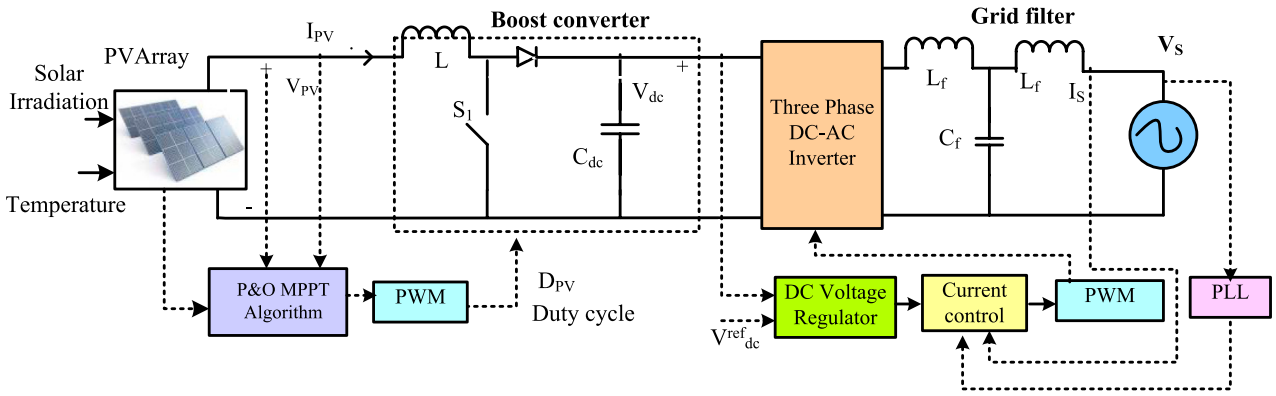

FIGURE 3
Solar with a boost converter and inverter control.

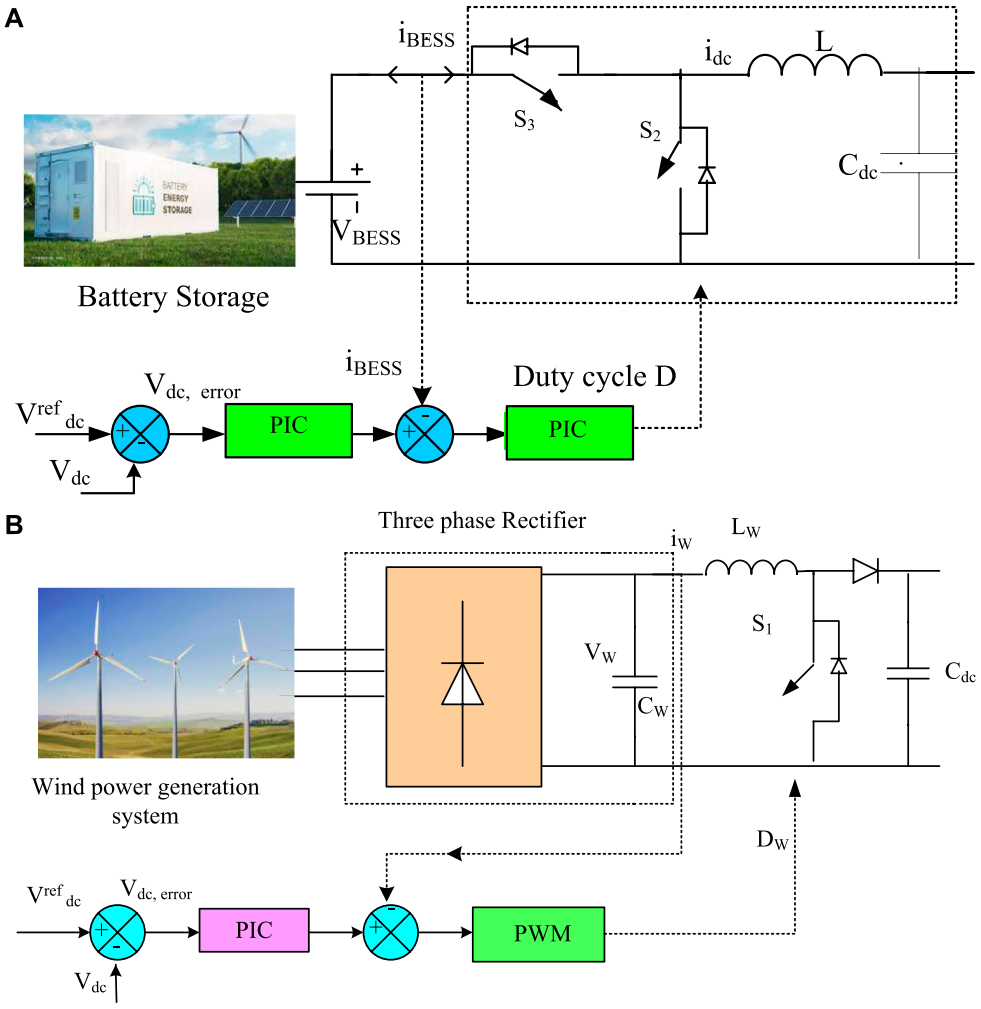

FIGURE 4
Battery and Wind control systems.

problems such as disturbances, swells, sags, and so on, through U-SWBEV.

- The incorporation of RES, EVs, and BESS into the UPQC serves to alleviate the strain on VSC, provides support for meeting load requirements, and ensures the steady maintenance of the stable voltage across DC link, even amidst variations in irradiation, wind velocity and load.

Furthermore, the proposed system was evaluated across four test scenarios involving varying loads, wind velocity and

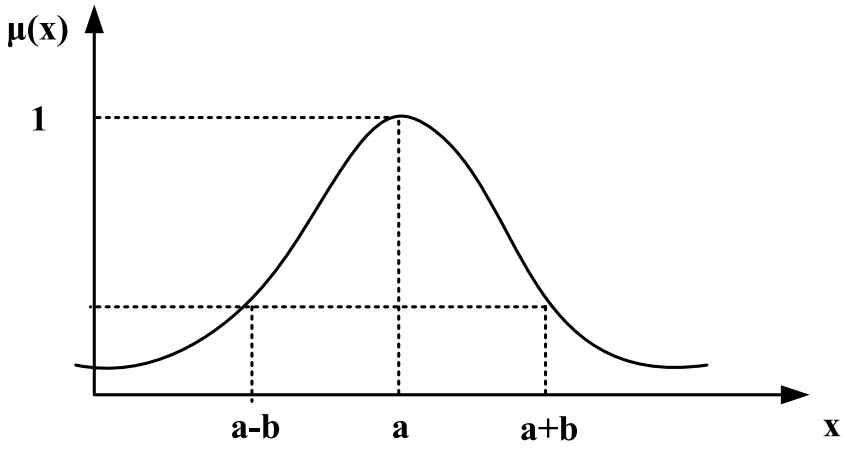

FIGURE 5
Gaussian MSF.

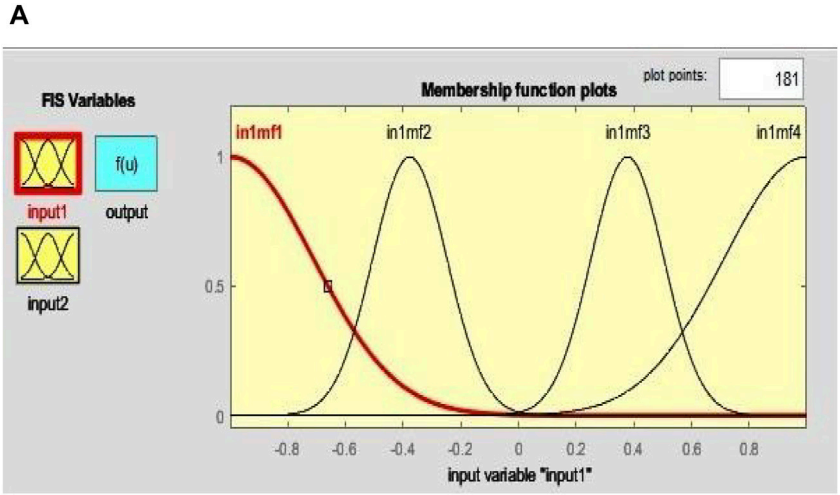

MSF of input-1

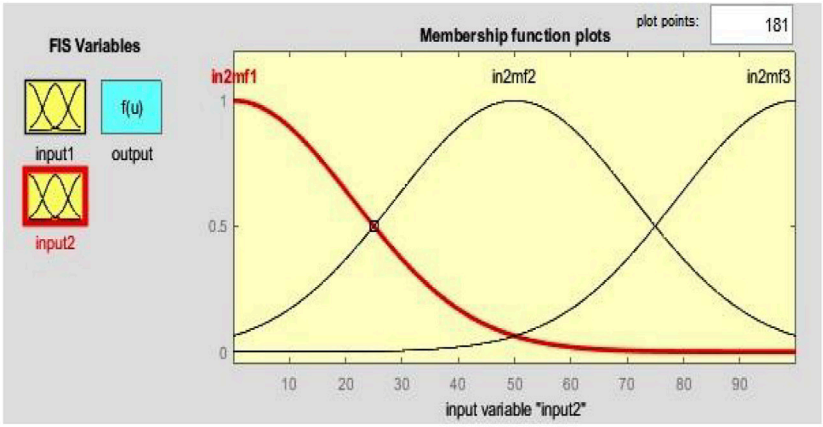

MSF of input-2

FIGURE 6
MSF for power management.

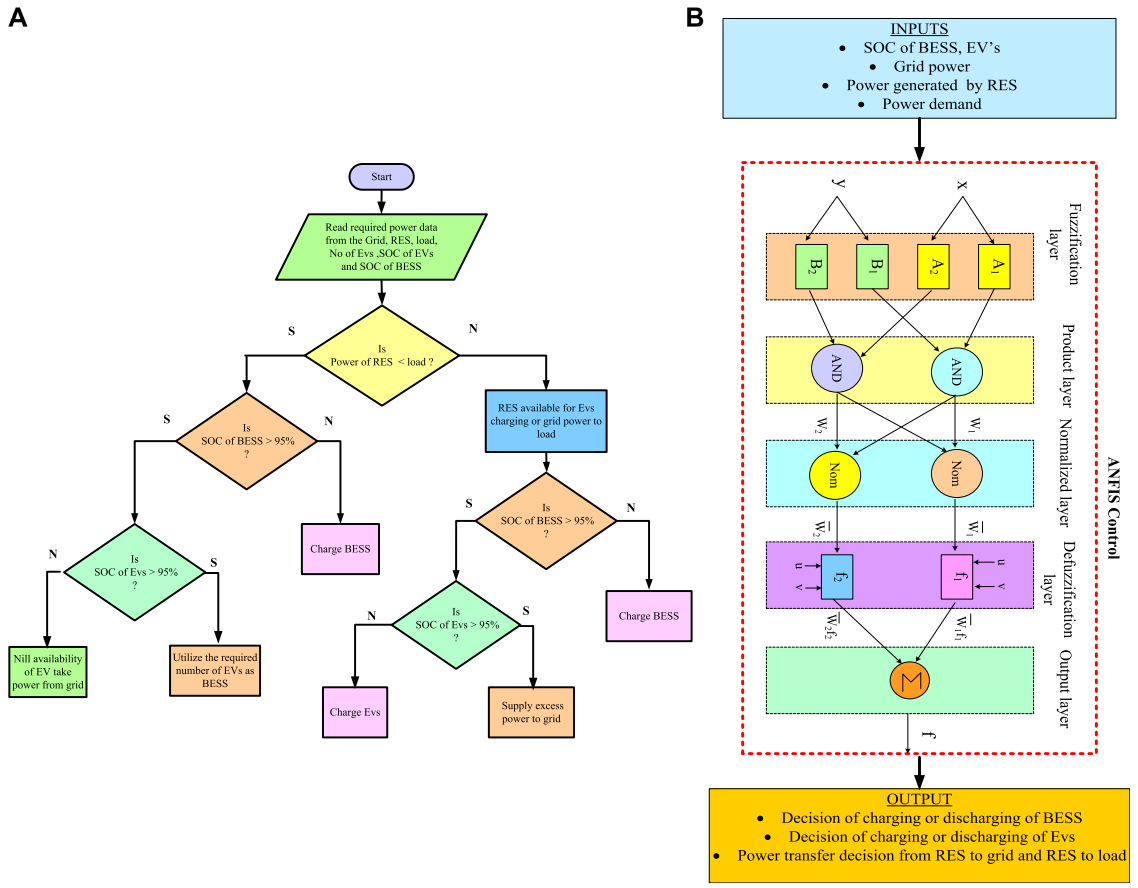

FIGURE 7
Power management.

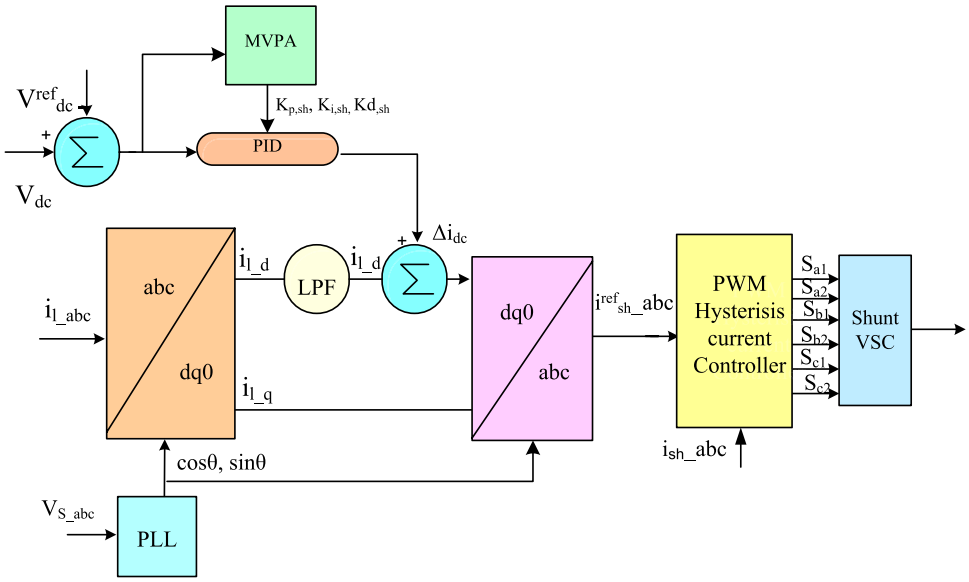

FIGURE 8
Shunt controller converter system.

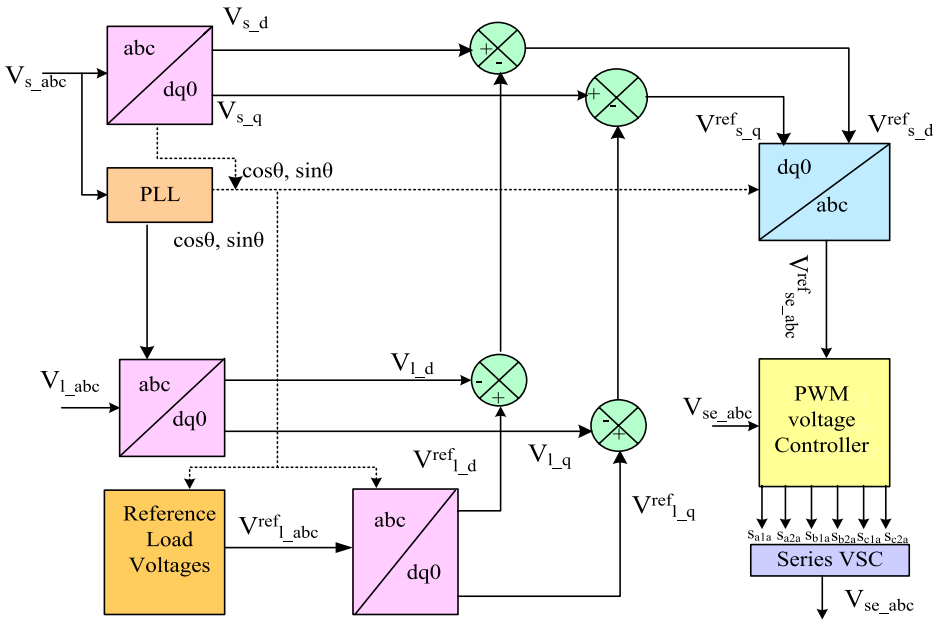

FIGURE 9
Series controller converter system.

irradiation circumstances. This assessment demonstrated its outstanding achievement in minimizing THD in current waveforms and reducing voltage waveform fluctuations. The system's performance was assessed through comparisons with the GA, PSO and ACO techniques.

The paper's organization is as follows: Section II delves into the modeling of U-SWBEV, while Section III provides the application of the techniques utilized in this study, focusing on the ANFIS and EMVPA. Section IV presents the results along with accompanying discussions. Lastly, Section V summarizes the conclusions drawn from the proposed work and provides the potential directions for future research in this field.

2 Proposed U-SWBEV

The suggested system's schematic arrangement is depicted in Figure 1. WES, SPV, BESS, and EV grid connection allows for parallel power flow management and PQ control. The series filter's main job is to take care of grid-side voltage-related problems. This is accomplished by supplying the necessary V_{se}, which is supplied via the interfacing transformer together with the appropriate choice of L_{se}. The shunt filter is linked to the grid through L_{sh} in a similar way. The SHAPF's job is to lower the harmonics in the current by adding compensating currents and preserving a steady DLCV. The primary benefit of external renewable source support lies in the reduction of the necessary converter ratings and the alleviation of converter stress. The parameters chosen for SPV, WES, BESS, and EVs can be found in Table 2. The power flow is determined using Eq. 1.

$$P_{PV} \pm P_{BESS} + P_w \pm P_{EV} + P_{Grid} = P_L \quad (1)$$

2.1 SPV structure

SPV technology harnesses sunlight to generate electricity, with its effectiveness contingent upon the configuration of PV modules interconnected in both series and parallel. PV modules are organized in a series arrangement to form what is known as a string, these strings are further linked in parallel to attain the required voltage and current levels. Each PV cell within a module is represented by a single-diode equivalent circuit, as illustrated in Figure 2. The control system of the SPV system with the boost converter is shown in Figure 3.

Thei_{ph} is obtained by Eq. 2, and PV module reverse saturation current i_{rs} is given by Eq. 3

$$i_{ph} = [i_{SC} + K_i(T - 298)]^* G/1000 \quad (2)$$

$$i_{rs} = i_{SC}/[\exp(qV_{oc}/N_s \eta k T) - 1] \quad (3)$$

The module saturation current depends on cell temperature, which is given by Eq. 4 and the output current of the module is given by Eq. 5

$$i_{mo} = i_{rs}[T/T_n]^3 \exp\left[q^* E_g/\eta k(1/T - 1/T_n)\right] \quad (4)$$

$$i_{PV} = N_p{}^* i_{ph} - N_p{}^* i_{mo}{}^* \left[\exp\left(V_{pv}/N_s + i_{PV}{}^*(R_{s,PV})/\eta V_t\right) - 1\right] - i_{sh,PV} \quad (5)$$

The P_{PV} is evaluated by Eq. 6.

$$P_{PV} = V_{PV} \times i_{PV} \quad (6)$$

2.2 BESS

The BESS plays a vital role in power management, ensuring the fulfillment of load demands. Batteries, cells are arranged in either series and or parallel, are employed to achieve the

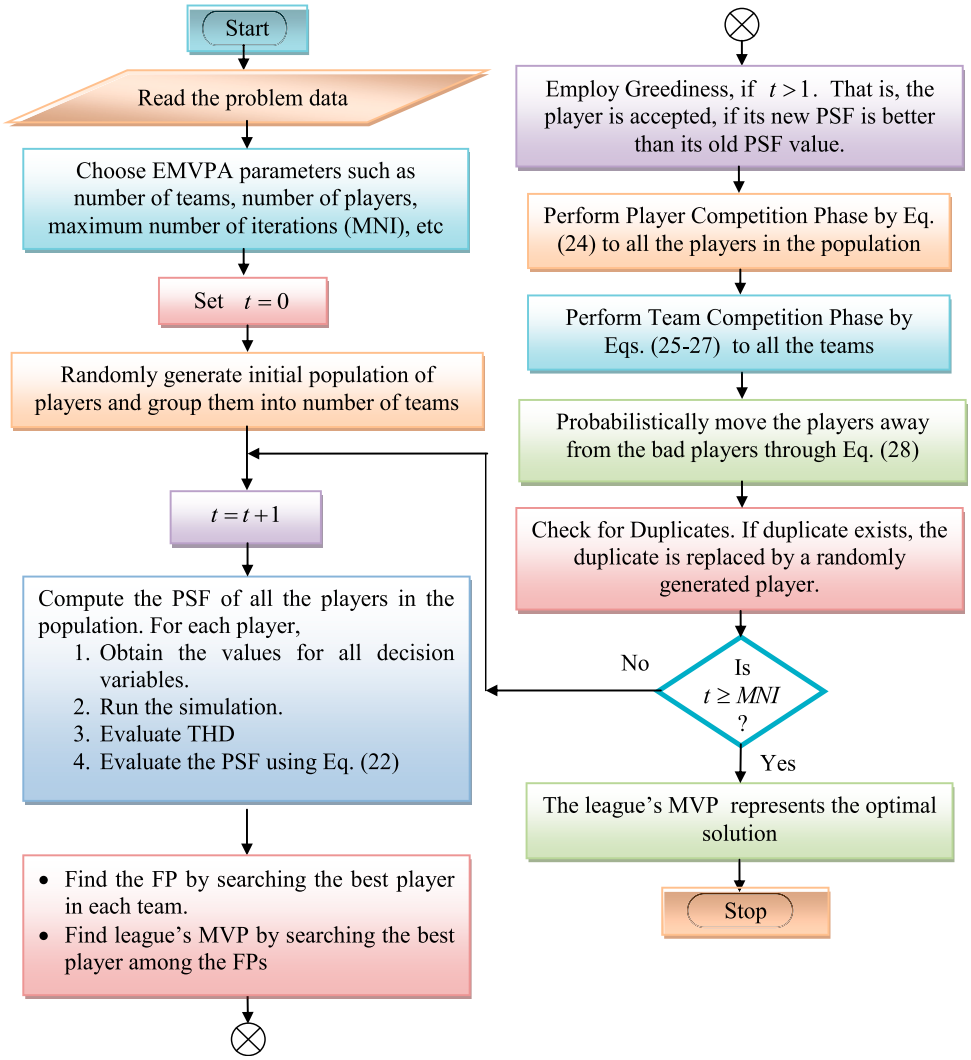

FIGURE 10
Flow of the filter parameters selection using EMVPA.

necessary current and voltage levels. The battery control system with a Buck-boost converter is illustrated in Figure 4A. The BESS also contributes to stabilizing the DLCV. The voltage and current requirements determine the specific arrangement of cells in the battery. For this research, a Li-ion battery has been chosen from the Simulink library. The *SOC* is represented in Eqs 7, 8.

$$SOC = 95\left(1 + \int i_{BSS}\, dtQ\right) \tag{7}$$

$$SOC_{\min} \leq SOC \leq SOC_{\max} \tag{8}$$

2.3 Wind system

By rectifying, the AC voltage generated by the WES is transformed into DC voltage, which is then raised with the aid of a boost converter that boosts the voltage. In this study, a permanent magnet synchronous machine is taken into consideration because of its dependability, affordability, ease of management, and superior performance. In Figure 4B, the WES controller is displayed. The power produced by WES can be found in Eqs 9–13.

$$R_{st} = \omega R_b / V_w \tag{9}$$

$$P_{mop} = 0.5\rho\pi R^{2_b} C_{pc} V^3 \omega \tag{10}$$

$$P_{mop} = \omega\, T_{mop} \tag{11}$$

$$C_p = \left(0.44 - 0.0167\theta_p\right) \sin \frac{3.14\,(N_r - 2)}{13 - 0.3\theta_p} \tag{12}$$

$$-0.0018\,(N_r - 2) = \theta_p \tag{13}$$

3 ANFIS power flow management

The ANFIS controller utilizes the RES power generation forecasting system and load forecasting system to manage the

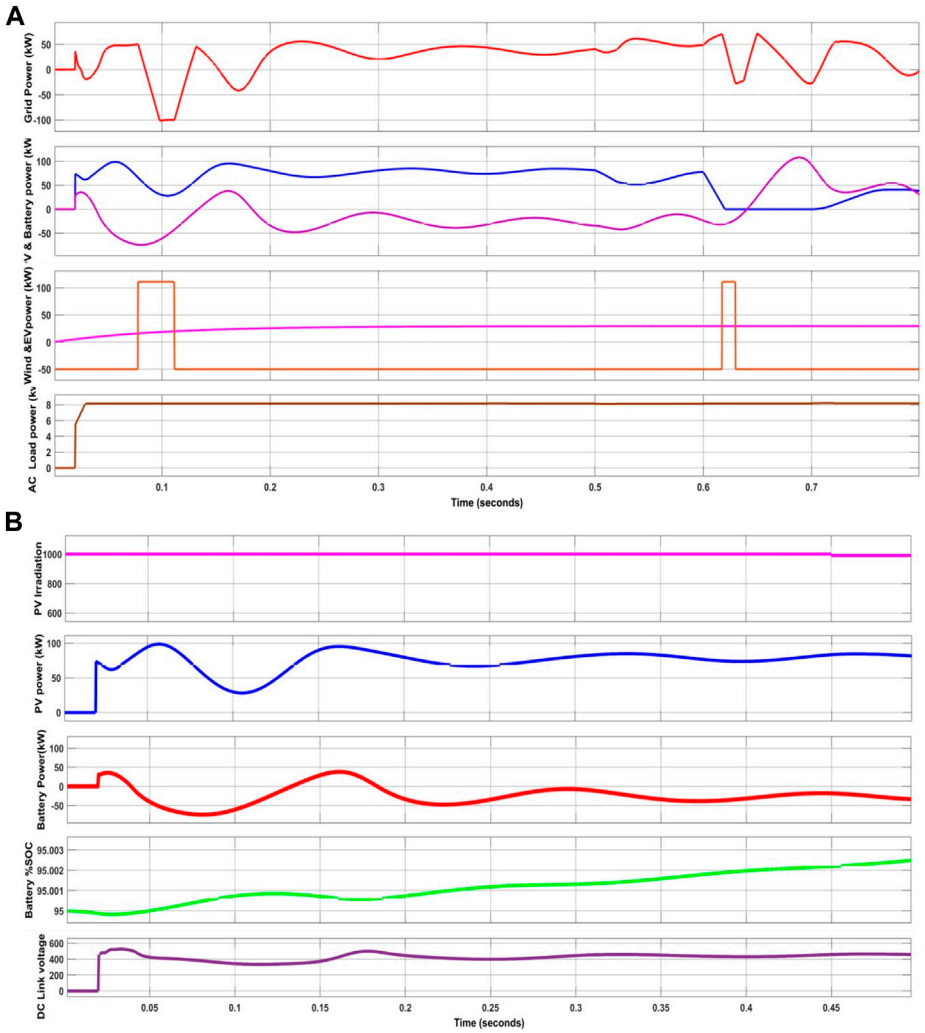

FIGURE 11
(Continued).

power exchange between EVs and the grid. It facilitates the transfer of power either from EVs to the grid or *vice versa*. This research offers insights into enhancing PQ in addition to power flow management in the grid system through the integration of EVs with UPQC. This highlights the primary objective of implementing ANFIS power flow management, which is to regulate the utilization of EVs as portable, temporary BESS. Consequently, when the stored energy is not needed, it can also be employed for transportation.

The ANFIS controller adapts the characteristics of an ANNC and an FLC. The inputs provided to the ANFIS are primarily calibrated based on the MSF to generate optimal results, as demonstrated in Figure 5. The ANFIS comprises of five layers, with the first layer being the Fuzzification layer, where the outputs consist of MSF as defined in Eq. 14.

$$\begin{aligned} &\mu_{Ai}(x), i = 1, 2. \\ &\mu_{Bj}(y), j = 1, 2. \end{aligned} \tag{14}$$

Here, $\mu_{Ai}\ \mu_{Bj}$ represents the outputs derived from the MSF in the first layer. The Gaussian MSF is represented in Eq. 15.

$$\mu(x) = e^{-\left(\frac{x-a}{b}\right)^2} \tag{15}$$

Moreover, in the second layer (where fuzzy rule weighting is performed), the AND logic is utilized to compute the firing capability w_i by considering the MSF generated in the first layer, the output of which is determined using Eq. 16.

$$w_k = \mu_{Ai}(x)^* \mu_{Bj}(y) i, j = 1, 2. \tag{16}$$

In the third layer, values received from the preceding layer undergo normalization. Each node in this layer achieves normalization by calculating the kth rule's truth value to the total summation of firing strengths, as described in Eq. 17.

$$\overline{w_k} = \frac{w_k}{w_1 + w_2} k = 1, 2. \tag{17}$$

The ANNC's ability to self-adapt is executed through the application of the inference variables (p_k, q_k, r_k) in the fourth layer, which produces an output as defined in Eq. 18.

$$\overline{w_i} f_i = \overline{w_i}\left(p_k u + q_k v + r_k\right) \tag{18}$$

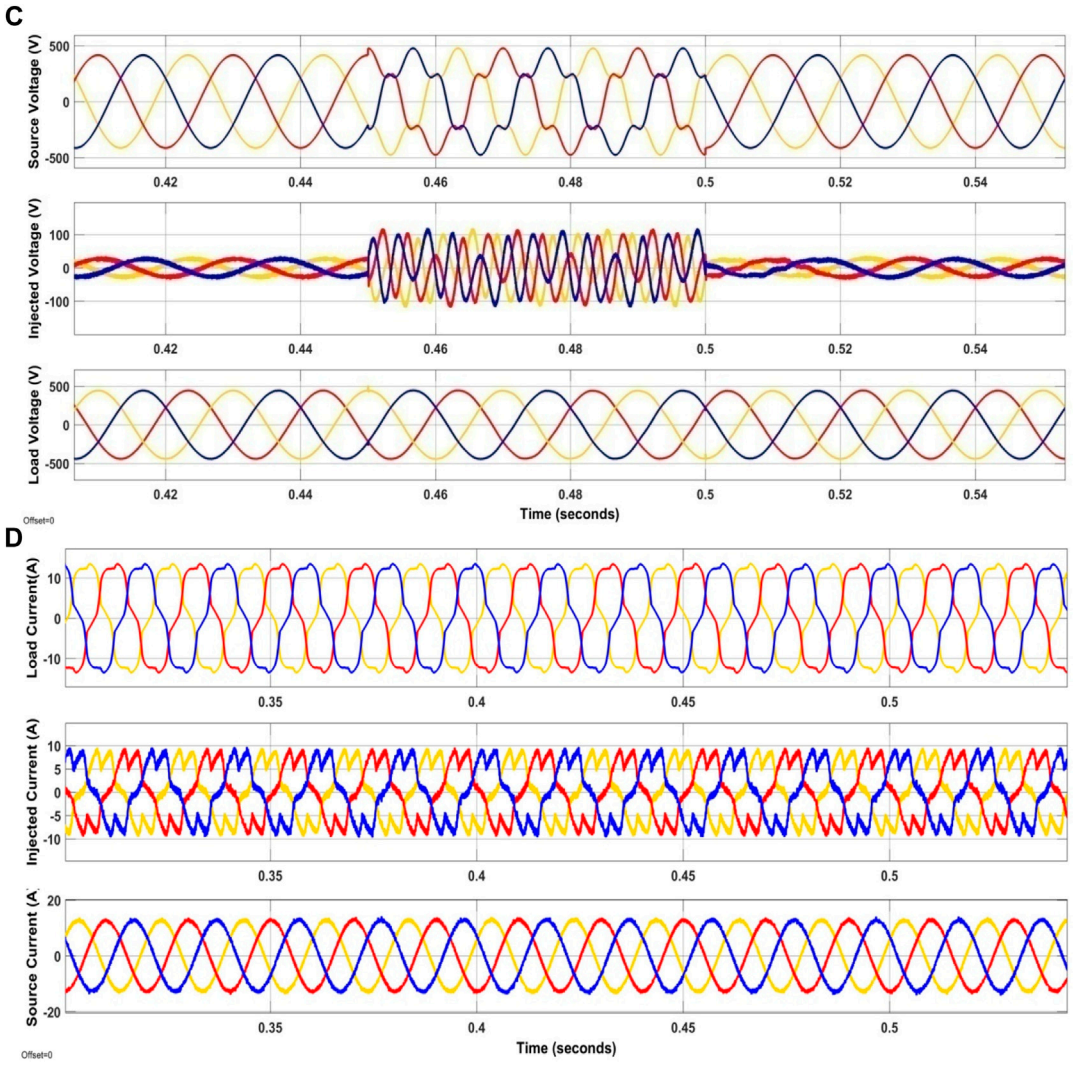

FIGURE 11
(Continued). Waveforms of the developed method for case1.

Finally, in the fifth layer, the inputs are aggregated to yield the ultimate desired output of the ANFIS, as indicated in Eq. 19. Figure 6 illustrates the configuration of the suggested ANFIS, and the Membership Function (MSF) for input 1 and input 2.

$$f = \sum_i \overline{w_i} f_i \tag{19}$$

In this work, the effective management of power flow is handled by ANFIS. Power flow occurs between the various entities, including the grid, RESs, BESS, and charging stations and load by ANFIS regulator. However, this plays a pivotal role in making decisions about EV charging. When EVs are not in use, they can be stationed at charging stations.

These EVs can also function as BESS during high load periods, which results in a reduction of the grid's peak load hour. The contribution of EVs and their SOCOB play a significant role in determining the amount of power they can provide to the grid. The operational process of the proposed power flow is explained through the flowchart presented in Figure 7A. The developed ANFIS-based power management system is visually depicted in Figure 7B.

4 Shunt and series controllers of UPQC

The shunt SVC to mitigate harmonics in the supply current and regulate the DLCV employs the dq0-abc transformation and its inverse with the optimally tuned PIDC using EMVPA. The PLL provides frequency and phasor information from the supply voltage to transfer the current at load terminals into dq0 components. The PIDC continually compares the actual DC voltage with a set reference voltage to provide stable DC voltage, making necessary current adjustments to correct any deviations. The *d*th component of the load current is integrated into the PIDC control. Gate signals are generated using a Hysteresis controller, as depicted in Figure 8.

After converting from the abc-dq0 domain and then converting back to the abc domain, the terminal voltage is compared to a predetermined reference voltage. This comparison process then

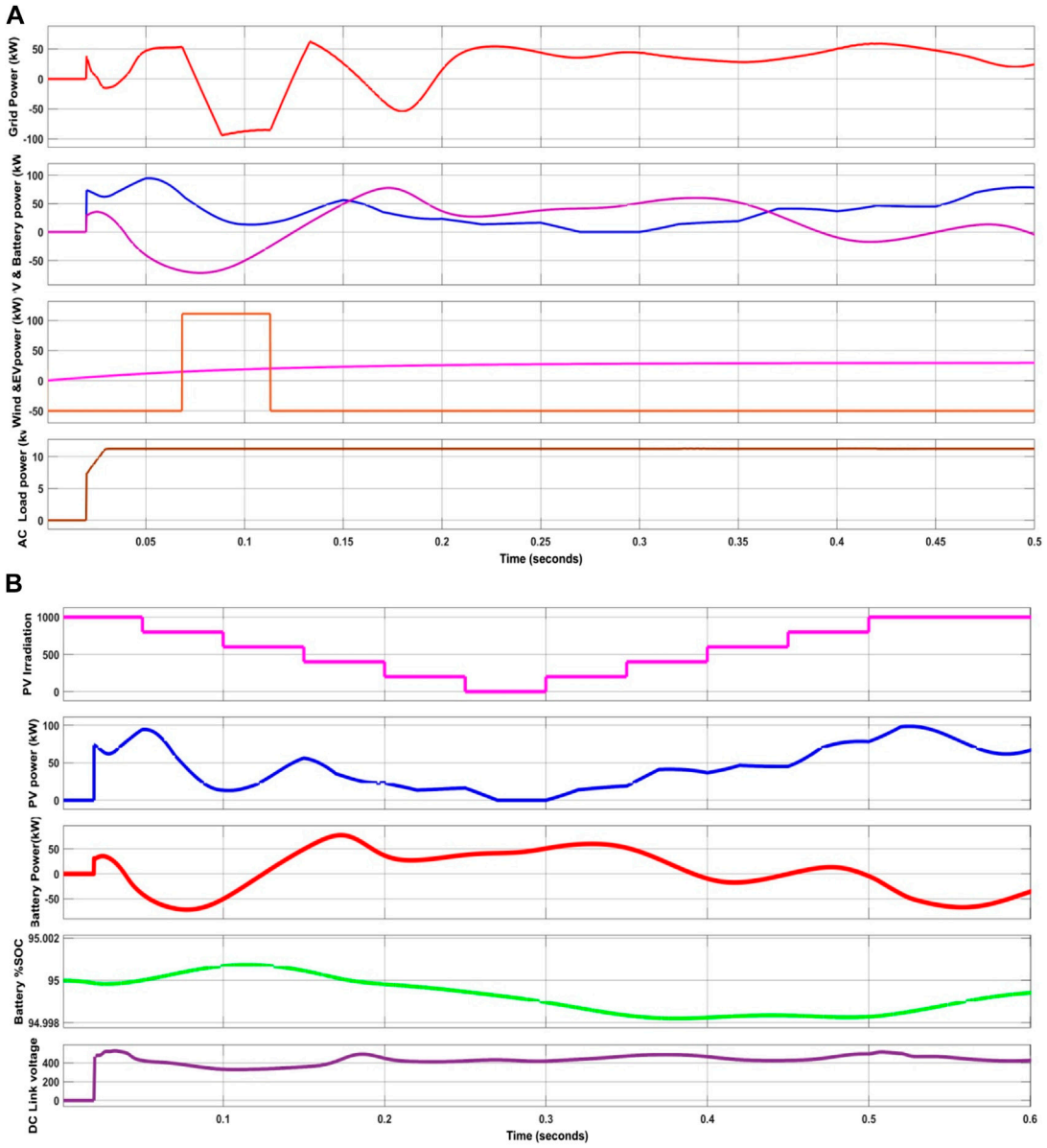

FIGURE 12
(Continued).

leads to the production of the essential gate current pulses for the series converter, as depicted in Figure 9. These current signals serve as the trigger pulses for the execution of PWM within the series converter.

4.1 EMVPA for optimal selection of PID controller gain values and filter parameters

The method proposed, known as EMVPA, encompasses the following key steps: (i) the creation of players (PLs), (ii) the establishment of a PSF, and (iii) the implementation of an "Avoidance of Bad PLs" approach to enhance the resilience of the existing EMVPA.

4.1.1 Players representation

The EMVPA is an algorithm rooted in swarm intelligence, drawing inspiration from sports games. In such games, a collective of PLs competes in multiple teams with the aim of achieving the championship title. Each PL within these teams plays individually with the ultimate objective of earning the MVP award. The set of PLs $\{P_1, P_2, \cdots, P_{nP}\}$ is initially distributed randomly to create multiple teams $\{\aleph_1, \aleph_2, \cdots, \aleph_{nT}\}$. The success of each PL within every team relies on their unique abilities and is measured using score. The player designated as *i*th, possessing a range of skills, is mathematically denoted as a variable in the problem.

$$P_i = [skill_{i,1}, skill_{i,2}, \cdots, skill_{i,ns}] \tag{20}$$

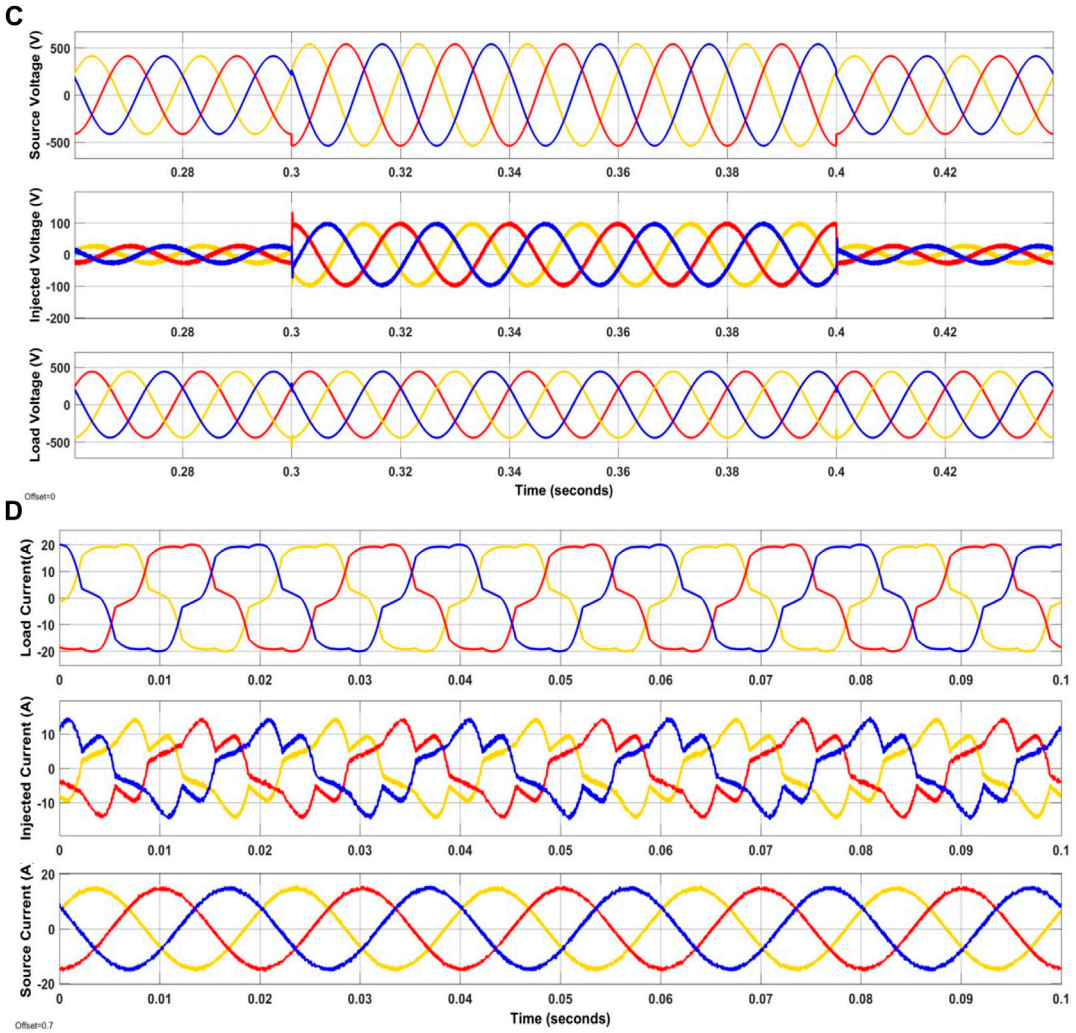

FIGURE 12
(Continued). Waveforms of the developed method for case2.

Each PL, with their unique skill set within the team, is symbolized to represent the gain values of the PIDC for the shunt controller, as well as the shunt and series filter parameters as control variables as defined in Eq. 21.

$$P_i = \left[K_p, K_i, K_d, R_{se}, R_{sh}, L_{se}, L_{sh}\right] \tag{21}$$

4.1.2 Performance score function

In most swarm-intelligence-based evolutionary algorithms, the performance of offspring is typically assessed using a FF. Since the EMVPA takes inspiration from sporting games where the victor is determined by their scores, the FF is referred to as the PSF. It is constructed from the objective of the problem selected while satisfying the constraint defined in Eq. 22, as follows:

$$\text{Maximize } PSF = \frac{1}{1 + THD} \tag{22}$$

Where, THD is evaluated by Eq. 23.

$$THD = \frac{\sqrt{(I^2{}_2 + I^2{}_3 + ...I^2{}_n)}}{I_1} \tag{23}$$

4.1.3 Competition among the players

Every PL within a team strives to boost their skills by engaging with their team's FP and the league's MVP with the goal of ascending to the role of their team's FP. The progression in skill enhancement during each iteration can be represented as follows:

$$\aleph_i = \aleph_i + rand \times (FP_i - \aleph_i) + C \times rand \times (MVP - \aleph_i) \tag{24}$$

Where, the constant C can be chosen as any integer value depending on the nature of the algorithm chosen for optimization.

4.1.4 Competition among the teams

Here, $\aleph_i$ team engages in a competition against a arbitrarily chosen opposing $\aleph_j (i \neq j)$ team. The probability of $\aleph_i$ team defeating team $\aleph_j$ is assessed as follows:

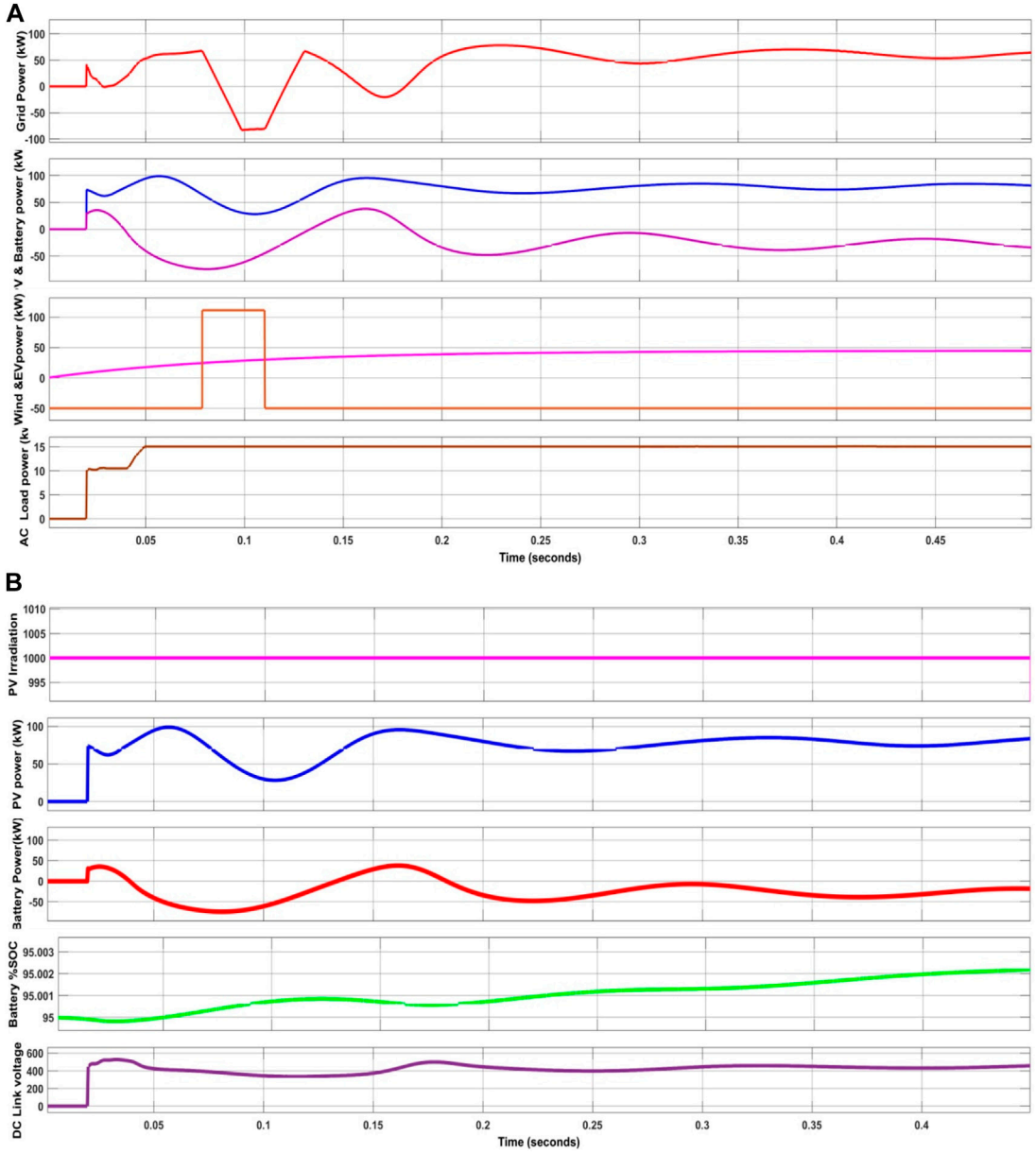

FIGURE 13
(Continued).

$$prob\left\{\aleph_i \text{ beats } \aleph_j\right\} = 1 - \left[\frac{\mathrm{PSF}(\aleph_i)^k}{\mathrm{PSF}(\aleph_i)^k + \mathrm{PSF}\left(\aleph_j\right)^k}\right] \quad (25)$$

Here, "k" denotes the winning probability and is set to 1, while $PSF(\aleph_i)$ represents the PSF of the selected PL in team $\aleph_i$. When team- $\aleph_i$ emerges as the victor in the game, the skills of the PLs in $\aleph_i$ undergo improvement as follows:

$$\aleph_i = \aleph_i + rand \times \left(\aleph_i - FP_j\right) \quad (26)$$

Otherwise, the skills of the PLs in $\aleph_i$ are improved as follows:

$$\aleph_i = \aleph_i + rand \times \left(FP_j - \aleph_i\right) \quad (27)$$

4.1.5 Escaping from bad players

The optimization process of the EMVPA can be further improved by considering the avoidance of suboptimal traps, particularly by identifying and mitigating the influence of underperforming players on the team. In sports physical contact between PLs can lead to injuries can result in PLs having to retire from the sport.

Even though various strategies were implemented to reduce injuries like helmet, pads, *etc.* Nevertheless, PLs in team sports tend to naturally avoid confrontations with aggressive or reckless PLs, maintaining distance to avoid contact-related injuries. This tendency of escaping problematic PLs can be adapted into the MVPA, with the aim of steering clear of

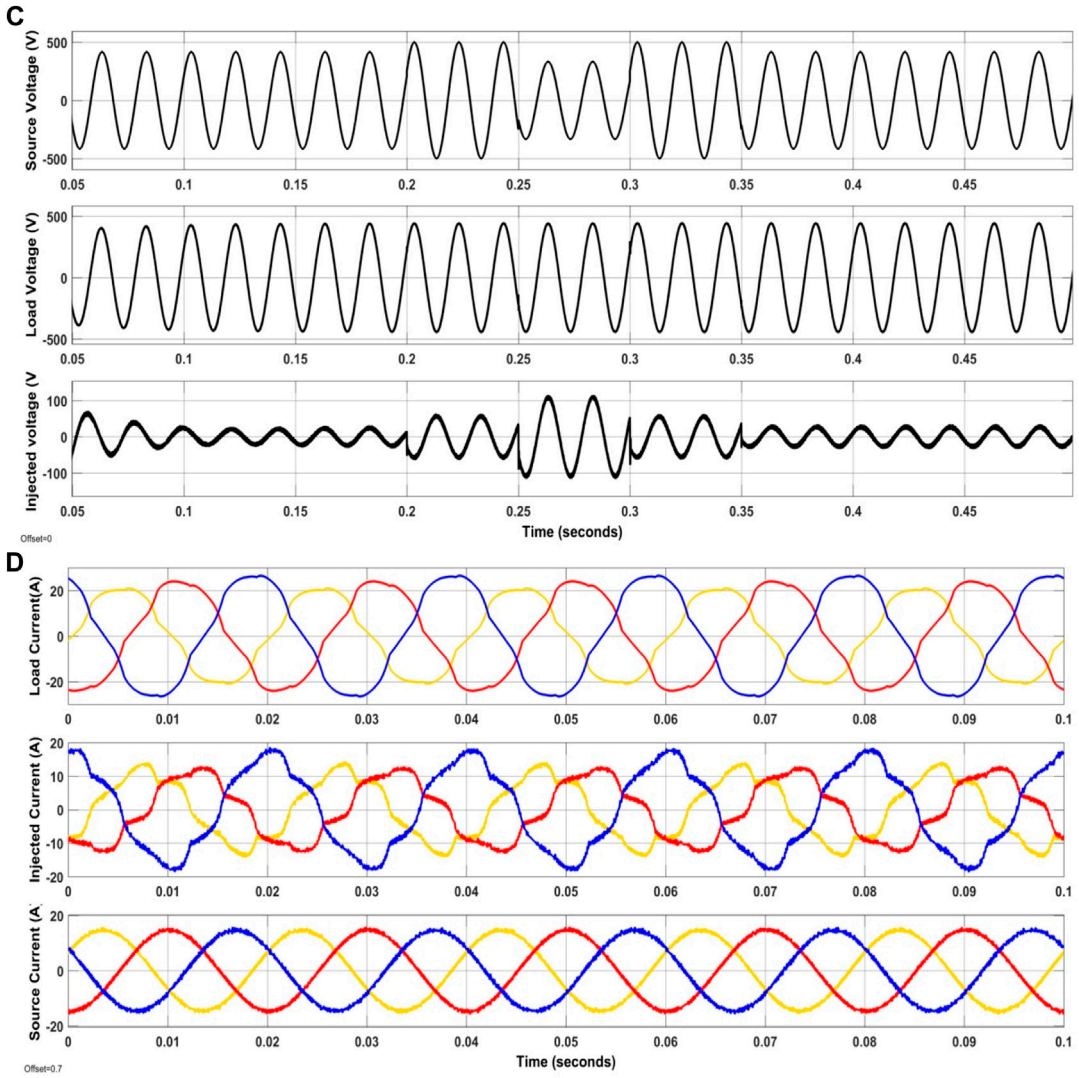

FIGURE 13
(Continued). Waveforms of the developed method for case3.

suboptimal outcomes by increasing the γ between each player and those deemed as subpar. This escaping mechanism can be implemented as follows:

$$\begin{aligned} P_i &\leftarrow P_i + \alpha.e^{-\gamma}, \quad if\ \gamma > 0 \\ P_i &\leftarrow P_i - \alpha.e^{+\gamma}, \quad if\ \gamma < 0 \end{aligned} \tag{28}$$

The described mechanism empowers PLs to steer clear of suboptimal solution points within the search space, bolstering their exploration capabilities and assisting the team in reaching the globally optimal solution.

4.1.6 Greediness

Following the sequence of PLs competitions, team competitions, and the avoidance of underperforming PLs by all team members, a greedy approach is applied to the PLs. This means that a new PL is accepted into the team only if their PSF is superior to the PSF value of the existing PL before the competition.

4.1.7 Solution process

An initial population of players, $\{P_1, P_2, \cdots, P_{nP}\}$, is generated by assigning random values within their respective bounds. These PLs are then randomly organized into multiple teams $\{\aleph_1, \aleph_2, \cdots, \aleph_{nT}\}$. The values of each PL, which represent the control variables for the PQ issue, are established as follows: parameters of PIDC, resistance and inductance values of filters. Subsequently, the PSF value for each player is computed after running simulink. This process is carried out for all PLs across all teams. Within each team, the player with the highest PSF value is recognized as the FP. Among all the FPs, the PL with the highest PSF value is bestowed with the title of the league's MVP. The PL and team competition

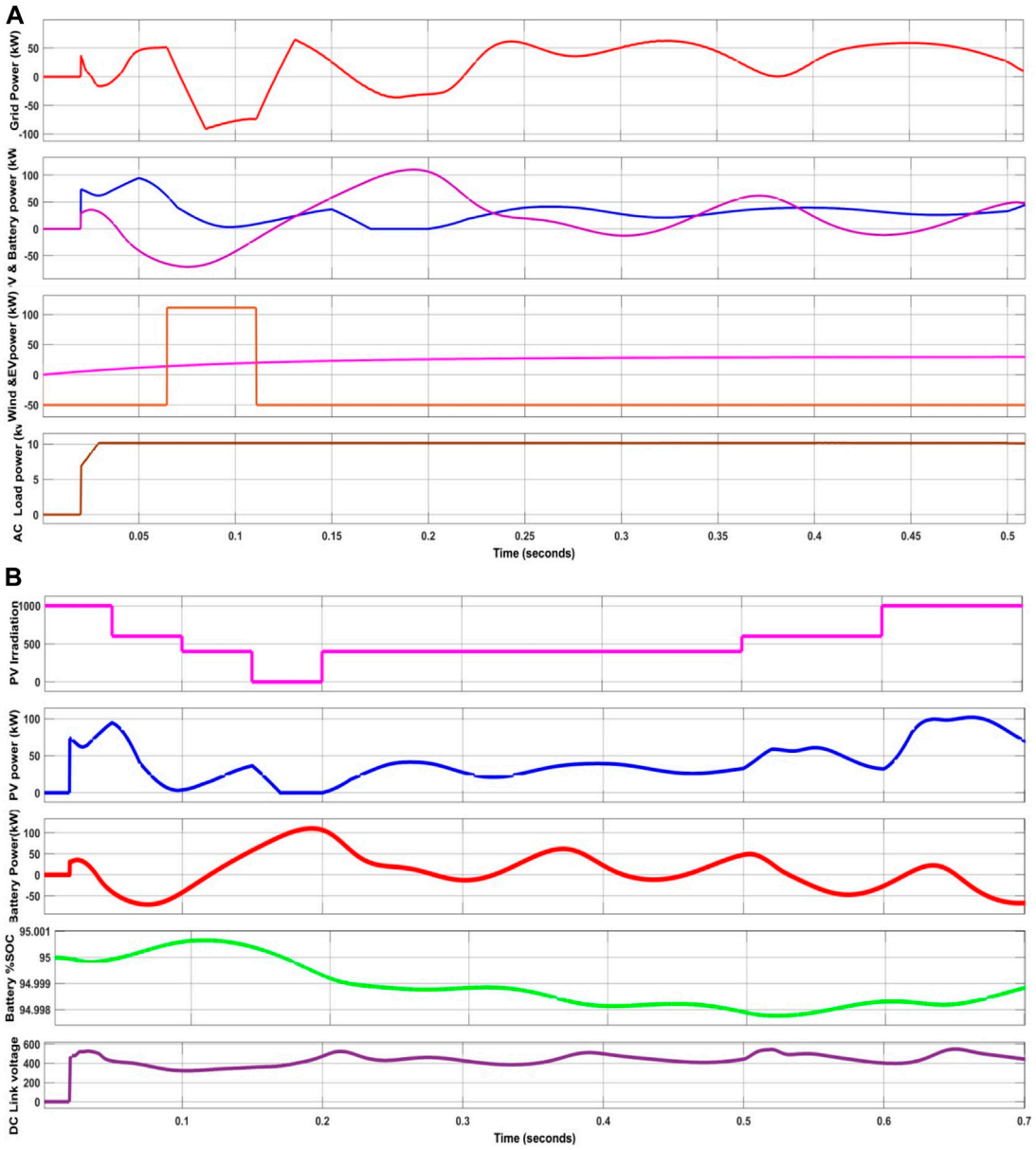

FIGURE 14
(Continued).

phases are initiated, following Eqs 24–27. The performances of the PLs are improved by mathematically distancing themselves from PLs that are considered "bad", as explained in Eq. 28.

The entire process, consisting of (i) computing PSF values, (ii) identifying FPs and the MVP, (iii) conducting PL competitions, team competitions, and avoiding bad PLs, constitutes a single iteration. The iterative cycle is repeated for a predetermined number of iterations, and the MVP at the point of convergence is identified as the global optima. Notably, the inclusion of a new player is contingent on their PSF value surpassing their previous PSF value. Moreover, the algorithm is designed to prevent ties, ensuring that in cases where two players attain an identical PSF value, a single player is chosen as the winner through a probabilistic selection process. However, the EMVPA was selected due to its advantages like fast convergence with lesser number of iterations with lower computational time for each iteration. Besides, the algorithm is having its own limitations like complexity due to which it is not preferable to solve multi objective engineering problems. In this work, the max number of iteration for termination is selected as 100 with 40 number of player in 4 teams (Srilakshmia et al., 2020). Figure 10 gives the visual representation of the proposed method's flowchart.

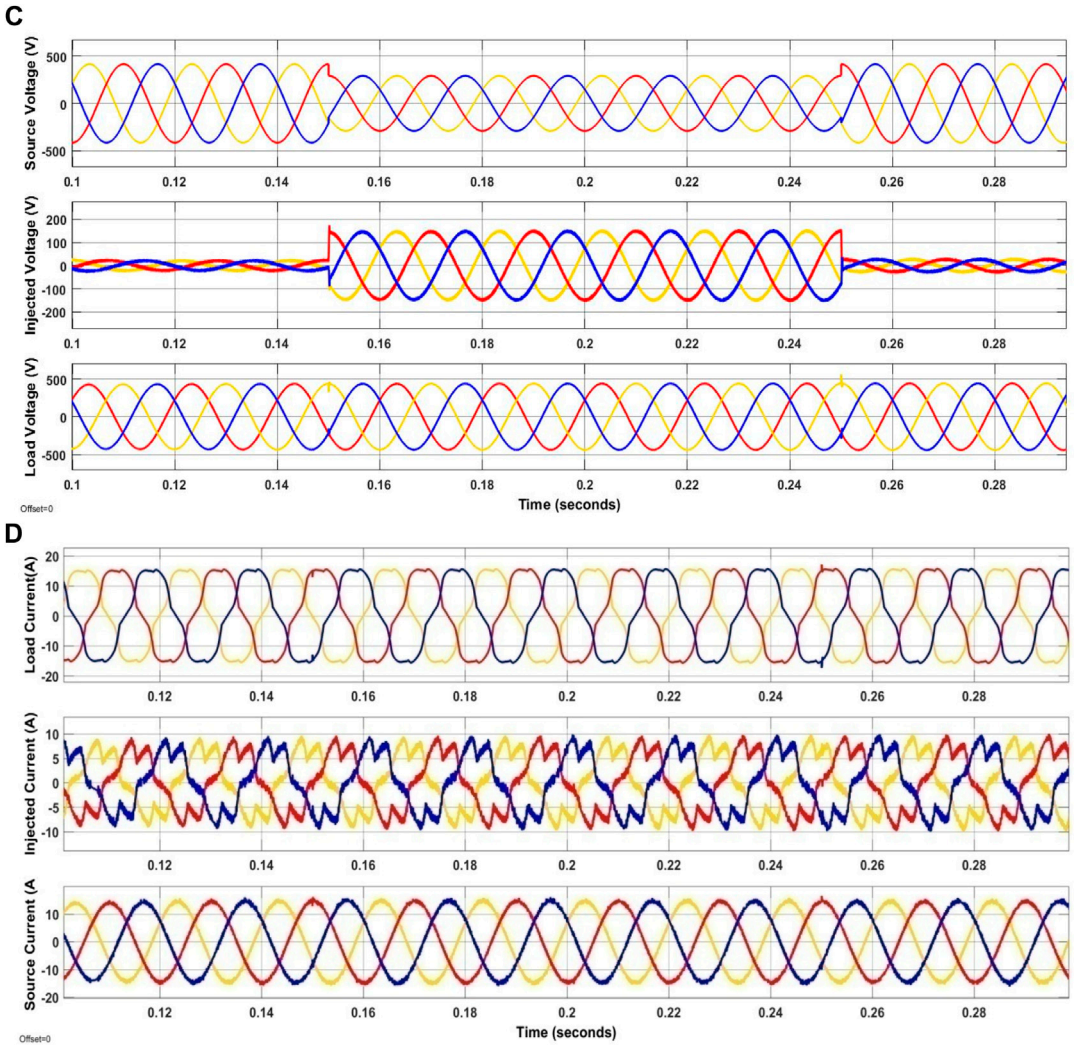

FIGURE 14
(Continued). Waveforms of the developed method for case4.

5 Results and discussions

The U-SWBEV integrated with ANFIS was developed and implemented using Simulink/Matlab 2022b. The simulation of the proposed system is visualized in Figure 16. The chosen system, as well as the selected parameters for the UPQC and the loads, is presented in Table 3 and Table 4. This study encompasses three distinct case studies given in Table 5, that involve various combinations of voltage-related problems such as sag, disturbance, and swell, along with scenarios that include fluctuating irradiation, wind velocity and a consistent temperature of 25°C. These case studies are employed to demonstrate the effectiveness of the developed ANFIS integrated with U-SWBEV. The primary objective of this work revolves around intelligent power flow management with a focus on effectively addressing PQ issues. This objective is achieved through the utilization of the ANFIS based power management and the UPQC for enhancing PQ.

As seen in Figure 11A for case 1, the suggested ANFIS is successfully handling EVSs in accordance with their SOCs. At this point, the grid draws power at 0.1 s while wind and PV provide their outputs. But in this scenario, BESS charge and EVs discharge (vehicle to the grid), delivering the required amount of power demand. Similarly, the grid provides power at 0.4 s when EVs are charging and PV, wind, and BESS provide their outputs. Here, RES provides power to the load in conjunction with the grid (grid to the vehicle). Furthermore, the constant irradiation and output power from the SPV system with a battery SOC of 95% are shown in Figure 11B in order to maintain stable DLCV. Next, Figure 11C shows how effectively the U-SWBEV series filter eliminates disturbances generated between 0.45 and 0.5 s by injecting the necessary voltage while aiming to keep the terminal voltage constant. Furthermore, as a result of the nonlinear load (the combination of loads 1 and 5), which causes the load current to be extremely polluted, the SHAPF provides the distortion free current to the supply by

TABLE 6 % THD comparison.

Case	Controller/Ref [ ]	%THD					
		Source current			Load voltage		
		Phase-a	Phase-b	Phase-c	Phase-a	Phase-b	Phase-c
1	PM with GA	4.98	5.01	4.68	1.48	1.43	1.39
	PM with PSO	4.78	4.98	4.77	1.46	1.37	1.30
	PM with ACO	4.57	4.65	4.73	1.34	1.32	1.35
	PM with EMVPA	**4.50**	**4.46**	**4.57**	**1.34**	**1.31**	**1.36**
2	PM with GA	3.98	3.77	3.56	1.47	1.41	1.39
	PM with PSO	3.91	3.68	3.87	1.35	1.31	1.39
	PM with ACO	3.82	3.47	3.51	1.47	1.33	1.34
	PM with EMVPA	**2.26**	**2.56**	**2.67**	**1.33**	**1.42**	**1.37**
	ANFIS Renduchintala et al. (2021)	2.43	--	--	--	--	--
	FLC Renduchintala et al. (2021)	6.13	--	--	--	--	--
	PIC Renduchintala et al. (2021)	14.74	--	--	--	--	--
	BF tuned PIC Sakthivel et al. (2015)	3.71	--	--	--	--	--
	ACO tuned PIC Sakthivel et al. (2015)	3.72	--	--	--	--	--
	PIC Sakthivel et al. (2015)	3.88	--	--	--	--	--
	PSO Mahaboob et al. (2019)	2.09	--	--	--	--	--
	HSO Mahaboob et al. (2019)	2.41	--	--	--	--	--
	ZN Mahaboob et al. (2019)	7.57	--	--	--	--	--
	ICM Mahaboob et al. (2019)	4.2	--	--	--	--	--
3	PM with GA	4.36	4.23	4.41	1.31	1.36	1.39
	PM with PSO	4.26	4.31	4.29	1.37	1.29	1.37
	PM with ACO	4.11	4.31	4.24	1.34	1.31	1.32
	PM with EMVPA	**4.09**	**4.13**	**4.32**	**1.27**	**1.21**	**1.26**
4	PM with GA	3.99	4.21	4.36	1.35	1.35	1.38
	PM with PSO	4.01	3.99	3.78	1.31	1.33	1.42
	PM with ACO	4.22	4.02	3.99	1.31	1.30	1.35
	PM with EMVPA	**3.98**	**3.99**	**4.21**	**1.30**	**1.32**	**1.34**

[a]Note: PM, is proposed method with ANFIS, power flow management.
Bold values indicate to highlight the proposed method.

injecting the necessary amount of current, as shown in Figure 11D which in turn reduces THD to 4.50% and enhances PF to almost unity.

In case 2, it is noted that the suggested method continues to function well in spite of variations in load and irradiation. Here, the grid draws power at 0.1 s from Figure 12A, with RES giving their output powers but at lower levels. To supply the necessary quantity of power to the load, EVs are made to be in the discharging condition in this instance while the BESS is in the charging state. The variable irradiation taken into account in this case during the load change from case 1 to case 2 is depicted in Figure 12B. Additionally, as shown in Figure 12C, the U-SWBEV series filter effectively reduces swell from 0.3 to 0.4 s by injecting the necessary compensatory voltage while keeping the terminal voltage constant. Besides, because load 3 and load 5 are nonlinear, the load current is heavily contaminated. To mitigate this, a shunt filter injects the necessary current as shown in Figure 12D and reduces THD to 2.26% and to almost unity.

In this case-3, a constant solar irradiation level is chosen while the load varies. Specifically, at 0.025 s, load 1 and 2 is added, and at 0.03 s, load 4 is included. The performance of the

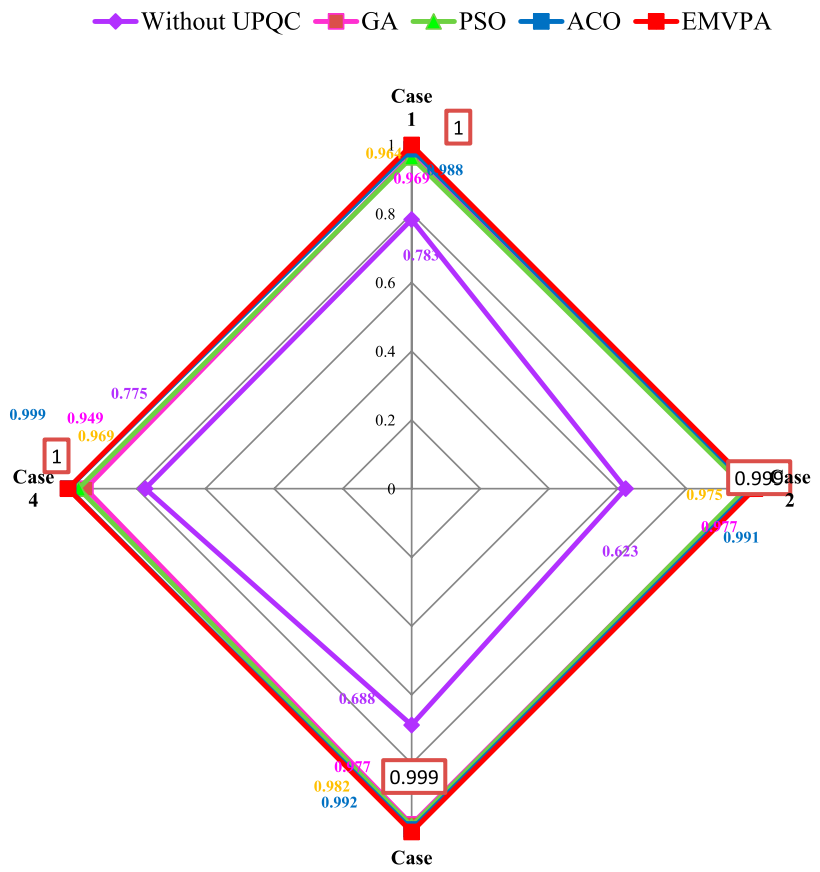

FIGURE 15
Comparison of PF.

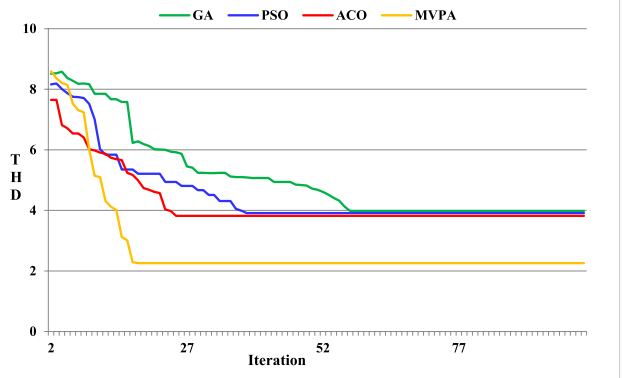

FIGURE 16
Comparison of convergence characteristics for case-1.

proposed method is seen in Figure 13A, which exhibits that the grid is under neutral state around 0.3 s. During this time, the RES supplies power to the load, while the BESS and EVSs are in the process of charging. Figure 13B displays the chosen constant solar irradiation alongside the power output and DLCV balancing. In this study, the voltage flicker situation is examined from 0.2 to 0.25 s which is efficiently mitigated by the UPQC. Additionally, the loads (in the combination of loads 1, 2 and 4), which leads to the unbalances and imperfections in the load current, the U-SWBEV handles effectively and provides sinusoidal source current with lower THD of 4.09% and enhances power factor to 0.999, as illustrated in Figures 13C, D.

In case 4, the variable solar irradiation is selected with load 1 at 0.025 s and load 2 at 0.03 s respectively. The performance of the proposed method can be seen in Figure 14A, where at 0.2 s, the grid is consuming power while the solar output is zero. The wind system, in conjunction with the BESS, supplies the necessary power to the load when EVSs are in the process of charging. Figure 14B illustrates the correlation between solar irradiation, PV power, BESS power, state of charge, and DLCV balancing. However, this study focused on the voltage sag condition occurring between 0.15 and 0.25 s. The compensation for this condition was efficiently achieved by the U-SWBEV, as illustrated in Figure 14C. In addition, the shunt filter effectively compensates for the polluted load current as depicted in Figure 14D, generated by rectified bridged non linear load and active power load which reduces THD to 3.98% which is much lesser that other methods listed in Table 6. Besides, it also boosts up the power factor to almost unity.

TABLE 7 Comparison of design parameters.

Case	Method	K_p	K_i	K_d	R_{se}	R_{sh}	L_{se}	L_{sh}
1	GA	44.631	63.741	1.124	1.362	0.165	8.365	8.997
	BBO	2.417	10.365	0.599	4.321	0.245	4.321	0.125
	ACO	3.124	44.981	1.899	6.347	0.199	3.740	0.124
	EMVPA	2.417	7.998	15.365	1.960	0.165	1.124	0.010
2	GA	64.998	71.369	54.325	2.365	0.124	5.982	9.998
	PSO	2.147	49.324	4.368	1.998	0.478	1.981	5.112
	ACO	4.001	47.369	1.336	6.347	0.398	3.447	3.987
	PIC Sakthivel et al. (2015)	0.507	10.3	--	--	--	--	--
	ACO tuned PIC Sakthivel et al. (2015)	0.912	247.93	--	--	--	--	--
	BF tuned PIC Sakthivel et al. (2015)	0.843	288.5	--	--	--	--	--
	PSO Mahaboob et al. (2019)	2.1345	10.2581	--	--	--	--	--
	HSO Mahaboob et al. (2019)	3.7151	45.4126	--	--	--	--	--
	ZN Mahaboob et al. (2019)	0.019	0.00042	--	--	--	--	--
	ICM Mahaboob et al. (2019)	0.0455	0.064	--	--	--	--	--
	ABC Rajesh et al. (2021)	8.2270	0.0020	--	--	--	--	--
	GSA Rajesh et al. (2021)	9.6325	2.3020	--	--	--	--	--
	FA Rajesh et al. (2021)	9.2545	1.6580	--	--	--	--	--
	MFOA Rajesh et al. (2021)	8.8554	1.8569	--	--	--	--	--
	EMVPA	6.124	5.369	4.998	8.561	0.435	2.365	5.325
3	GA	45.321	29.347	3.897	8.997	0.112	1.771	4.654
	PSO	1.945	81.369	7.698	7.658	0.214	5.334	5.974
	ACO	2.124	77.324	9.471	6.338	0.198	4.698	8.012
	EMVPA	3.987	0.100	5.487	9.412	0.401	1.974	9.778
4	GA	47.965	45.213	45.369	8.554	0.012	3.447	6.163
	PSO	10.981	0.112	81.654	7.211	0.201	2.001	7.549
	ACO	2.101	51.369	71.365	6.873	0.214	1.980	8.916
	EMVPA	19.981	19.336	43.541	1.557	0.272	5.145	4.749

The THDs of the suggested technique in all case studies is displayed in Table 6. The results demonstrate that the suggested method has significantly lower THD compared to other strategies, including those found in existing literature, and it also meets the standards set by the IEEE. In addition, the suggested system PF has value that is very close to unity, which is demonstrated in Figure 15, when compared to other approaches. Furthermore, it has been demonstrated as shown in Figure 16 that the proposed U-SWBEV with EMVPA achieves convergence to a reduced THD of 2.26% within 18 iterations. In comparison, GA, PSO, and ACO require 57, 38, and 25 iterations respectively to achieve convergence. Besides, the obtained designed parameter values of U-SWBEV were listed in Table 7.

Figure 17 depicts the FFT analysis of the source current for all cases in the proposed system. The proposed EMVPA technique is applicable for the best selection of shunt and series filters parameters optimally to reduce the burden on converters in addition to the elimination of imperfections in the current and voltage waveforms due to harmonics. Besides, the complexity of the proposed system can be justified by the optimal selection of filter parameters in addition to the controller parameters in association with AI control techniques for the better optimal solution.

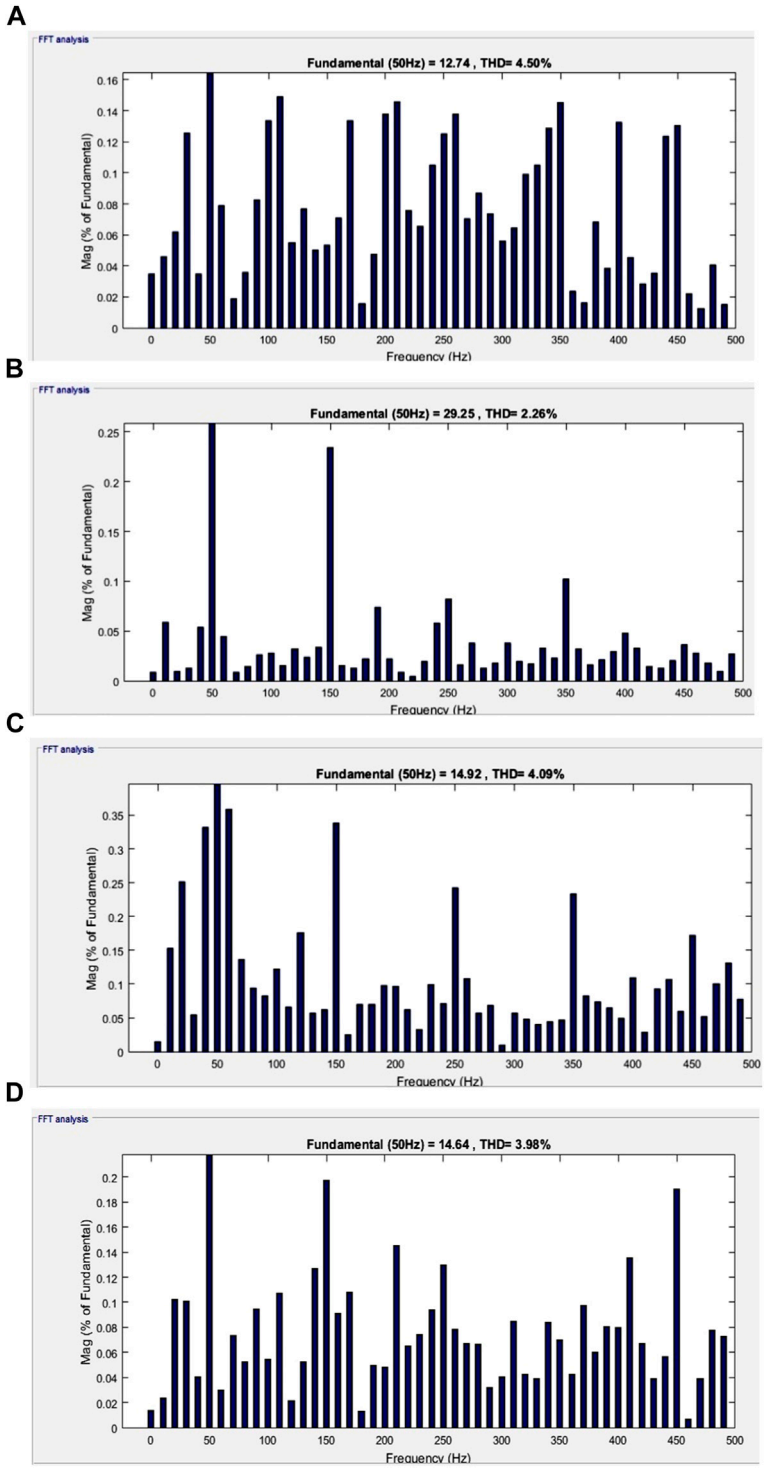

FIGURE 17
Current %THD spectrum for cases.

6 Conclusion

An intelligent ANFIS regulation is employed to effectively manage power flow in a system comprising Grid, RES, BESS and EVs. Here, UPQC is adopted to handle PQ issues to provide constant DC link voltage during varying loads, wind speeds, and irradiation conditions. In addition, the EMVPA method is employed to tune the gain values of PIDC, while also making an appropriate choice of filter parameters. The proposed power management system aims to meet the load demand and support

the required number of EVs. This work, simultaneously handles PQ issues and power management effectively. It effectively suppresses voltage disturbances, swells, sags, and defects in the current waveforms. However, with this proposed technique, the THD values for voltages and currents have been measured and found to be less than 5%. Future research can build upon the results of this study by incorporating metaheuristic algorithms to enhance the effective management of power flow even more.

Data availability statement

The original contributions presented in the study are included in the article/Supplementary Material, further inquiries can be directed to the corresponding author.

Author contributions

KS: Methodology, Writing–original draft. SG: Conceptualization, Software, Writing–original draft. SB: Formal Analysis, Writing–review and editing. PB: Writing–review and editing. GR: Investigation, Writing–review and editing. AP: Supervision, Writing–review and editing. SS: Funding acquisition, Writing–review and editing.

Funding

The author(s) declare that no financial support was received for the research, authorship, and/or publication of this article.

Conflict of interest

The authors declare that the research was conducted in the absence of any commercial or financial relationships that could be construed as a potential conflict of interest.

Publisher's note

All claims expressed in this article are solely those of the authors and do not necessarily represent those of their affiliated organizations, or those of the publisher, the editors and the reviewers. Any product that may be evaluated in this article, or claim that may be made by its manufacturer, is not guaranteed or endorsed by the publisher.

References

Amirullah, U. B., Surabaya, A., Adiananda, O., Penangsang, A., Soeprijanto, U. B., Surabaya, I. T. S., et al. (2020). Load active power transfer enhancement using UPQC-PV-BES system with fuzzy logic controller. *Int. J. Intell. Eng. Syst.* 2 (13), 329–349. doi:10.22266/ijies2020.0430.32

Ashok Kumar, L., and Indragandhi, V. (2020). Power quality improvement of grid connected wind energy system using facts devices. *Interanational J. Ambient Energy* 6 (41), 631–640. doi:10.1080/01430750.2018.1484801

Chellaswamy, C., and Ramesh, R. (2017). Future renewable energy option for recharging full electric vehicles. *Renew. Sustain. Energy Rev.* 76, 824–838. doi:10.1016/j.rser.2017.03.032

Elavarasan, R. M. (2020). 'Comprehensive review on India's growth in renewable energy technologies in comparison with other prominent renewable energy based countries. *J. Sol. Energy Eng.* 3 (142), 1–11. doi:10.1115/1.4045584

Ganesan, A., and Srinath, S. (2019). Optimal controller for mitigation of harmonics in hybrid shunt active power filter connected distribution system: an EGOANN technique. *J. Renew. Sustain. Energy* 11. doi:10.1063/1.5085028

Khosravi, N., Abdolmohammadi, H. R., Bagheri, S., and Miveh, M. R. (2021a). Improvement of harmonic conditions in the AC/DC microgrids with the presence of filter compensation modules. *Renew. Sustain. Energy Rev.* 143, 110898, 110898. doi:10.1016/j.rser.2021.110898

Khosravi, N., Abdolmohammadi, H. R., Bagheri, S., and Miveh, M. R. (2021b). A novel control approach for harmonic compensation using switched power filter compensators in micro-grids. *IET Renew. Power Gener.* 15, 3989–4005. doi:10.1049/rpg2.12317

Khosravi, N., Echalih, S., Baghbanzadeh, R., Hekss, Z., Hassani, R., and Messaoudi, M. (2022). "Enhancement of power quality issues for a hybrid AC/DC microgrid based on optimization methods," in *IET Renewable power generation*. doi:10.1049/rpg2.12476

Khosravi, N., Echalih, S., Hekss, Z., Baghbanzadeh, R., Messaoudi, M., and Shahideipour, M. (2023). A new approach to enhance the operation of M-UPQC proportional-integral multiresonant controller based on the optimization methods for a stand-alone AC microgrid. *IEEE Trans. Power Electron.* 38 (3), 3765–3774. doi:10.1109/TPEL.2022.3217964

Kong, P. Y., and Karagiannidis, G. K. (2016). Charging schemes for plug-in hybrid electric vehicles in smart grid: a survey. *IEEE Access* 4, 6846–6875. doi:10.1109/access.2016.2614689

Madurai Elavarasan, R., Afridhis, S., Vijayaraghavan, R. R., Subramaniam, U., and Nurunnabi, M. (2020a). SWOT analysis: a framework for comprehensive evaluation of drivers and barriers for renewable energy development in significant countries. *Energy Rep.* 6, 1838–1864. doi:10.1016/j.egyr.2020.07.007

Madurai Elavarasan, R., Selvamanohar, L., Raju, K., Vijayaraghavan, R. R., Subburaj, R., Nurunnabi, M., et al. (2020b). A holistic review of the present and future drivers of the renewable energy mix in Maharashtra, state of India. *Sustainability* 16 (12), 6596. doi:10.3390/su12166596

Mahaboob, S., Ajithan, S. K., and Jayaraman, S. (2019). Optimal design of shunt active power filter for power quality enhancement using predator-prey based firefly optimization. *Swarm Evol. Comput.* 44, 522–533. doi:10.1016/j.swevo.2018.06.008

Mansoor, M. A., Hasan, K., Othman, M. M., Noor, S. Z. B. M., and Musirin, I. (2020). Construction and performance investigation of three phase solar PV and battery energy storage system integrated UPQC. *IEEE Accesses* 8, 103511–103538. doi:10.1109/access.2020.2997056

Mirzapour, O., Karimi-Arpanahi, S., and Oraee, H. (2018). "Evaluating grid harmonics effect on induction motor using reduced thermal model," in 2018 Smart Grid Conference (SGC), Sanandaj, Iran, November 28th and 29th 2018, 1–5. doi:10.1109/SGC.2018.8777879

Mohamed, S. A. (2020). Enhancement of power quality for load compensation using three different FACTS devices based on optimized technique. *Int. Trans. Electr. Energy Syst.* 3 (30), 12196. doi:10.1002/2050-7038.12196

Nagireddy, V. V., Kota, V. R., and Ashok Kumar, D. V. (2018). Hybrid fuzzy back-propagation control scheme for multilevel unified power quality conditioner. *Ain Shams Eng. J.* 9 (4), 2709–2724. doi:10.1016/j.asej.2017.09.004

Nunes, P., and Brito, M. C. (2017). Displacing natural gas with electric vehicles for grid stabilization. *Energy* 141, 87–96. doi:10.1016/j.energy.2017.09.064

Okwako, O. E., Lin, Z.-H., Xin, M., Premkumar, K., and Rodgers, A. J. (2022). Neural network controlled solar PV battery powered unified power quality conditioner for grid connected operation. *Energies* 15 (2022), 6825. doi:10.3390/en15186825

Omid Mirzapour, Rui, X., and Sahraei-Ardakani, M. (2023). Transmission impedance control impacts on carbon emissions and renewable energy curtailment. *Energy* 278, 127741, 127741. doi:10.1016/j.energy.2023.127741

Paramanik, S., Sarker, K., Chatterjee, D., and Goswami, S. K. (2019). "Smart grid power quality improvement using modified UPQC," in Proc. Devices for Integr. Circuit (DevIC), Kalyani, India, 19-20 May 2021, 356–360.

Pazouki, S., and Haghifam, M.-R. (2021). Optimal planning and scheduling of smart homes' energy hubs. *Electr. Energy Syst.* 31, e12986. doi:10.1002/2050-7038.12986

Pazouki, S., and Olamaei, J. (2019). The effect of heterogeneous electric vehicles with different battery capacities in parking lots on peak load of electric power distribution networks. *Int. J. Ambient Energy* 40 (7), 734–738. doi:10.1080/01430750.2017.1423382

Rajesh, P., Shajin, F. H., and Umasankar, L. (2021). A novel control scheme for PV/WT/FC/battery to power quality enhancement in micro grid system: a hybrid technique. *Energy Sources, Part A Recovery, Util. Environ. Eff.*, 1–17. doi:10.1080/15567036.2021.1943068

Ramadevi, A., Srilakshmi, K., Kumar Balachandran, P., Colak, I., Dhanamjayulu, C., and Khan, B. (2023). Optimal design and performance investigation of artificial neural network controller for solar- and battery-connected unified power quality conditioner. *Int. J. Energy Res.* 2023, 1–22. Article ID 3355124. doi:10.1155/2023/3355124

Renduchintala, U. K., Pang, C., Tatikonda, K. M., and Yang, L. (2021). ANFIS-fuzzy logic based UPQC in interconnected microgrid distribution systems: modeling, simulation and implementation. *J. Eng.* 21 (1), 6–18. doi:10.1049/tje2.12005

Sakthivel, A., Vijayakumar, P., Senthilkumar, A., Lakshminarasimman, L., and Paramasivam, S. (2015). Experimental investigations on ant colony optimized pi control algorithm for shunt active power filter to improve power quality. *Control Eng. Pract.* 42, 153–169. doi:10.1016/j.conengprac.2015.04.013

Seyed Alizadeh, S. M., Bagherzadeh, A., Bahmani, S., Nikzad, A., Aminzadehsarikhanbeglou, E., and Tatyana Yu, S. (2021). Retrograde gas condensate reservoirs: reliable estimation of dew point pressure by the hybrid neuro-fuzzy connectionist paradigm. *ASME. J. Energy Resour. Technol. June* 144 (6), 063007. doi:10.1115/1.4052167

Shafiullah, G. M., Arif, M. T., and Oo, A. M. T. (2018). Mitigation strategies to minimize potential technical challenges of renewable energy integration. *Sustain. Energy Technol. Assessments* 25, 24–42. doi:10.1016/j.seta.2017.10.008

Srilakshmi, K., Krishna Jyothi, K., Kalyani, G., and Sai Prakash Goud, Y. (2023a). Design of UPQC with solar PV and battery storage systems for power quality improvement. *Cybern. Syst.*, 1–30. doi:10.1080/01969722.2023.2175144

Srilakshmi, K., Pandian, A. N., and Palanivelu, A. (2023b). Fuzzy based hybrid controller for UPQC with wind and battery storage systems. *Int. J. Electron.*, 1–26. doi:10.1080/00207217.2023.2245193

Srilakshmi, K., Srinivas, N., Balachandran, P. K., Reddy, J. G. P., Gaddameedhi, S., Valluri, N., et al. (2022a). Design of soccer league optimization based hybrid controller for solar-battery integrated UPQC. *IEEE Access* 10, 107116–107136. doi:10.1109/ACCESS.2022.3211504

Srilakshmi, K., Sujatha, C. N., Balachandran, P. K., Mihet-Popa, L., and Kumar, N. U. (2022b). Optimal design of an artificial intelligence controller for solar-battery integrated UPQC in three phase distribution networks. *Sustainability* 14 (21), 13992. doi:10.3390/su142113992

Srilakshmia, K., Ravi Babua, P., and Aravindhababub, P. (2020). An enhanced most valuable player algorithm based optimal power flow using Broyden's method. *Sustain. Energy Technol. Assessments* 42, 1008. doi:10.1016/j.seta.2020.100801

Vivas, F. J., Segura, F., Andújar, J. M., Palacio, A., Saenz, J. L., Isorna, F., et al. (2020). Multi-objective fuzzy logic-based energy management system for microgrids with battery and hydrogen energy storage system. *Electronics* 7 (9), 1074. doi:10.3390/electronics9071074

Zhao, X., Chai, X., Guo, X., Ahmad, W., Wang, X., and Zhang, C. (2021). Impedance matching-based power flow analysis for UPQC in three-phase four-wire systems. *Energies* 14 (2021), 2702. doi:10.3390/en14092702

Nomenclature

RES	Renewable energy sources
PIDC	Proportional integral derivate controller
PQ	Power quality
UPQC	Unified PQ Conditioner
EMVPA	Enhanced most valuable player algorithm
SPV	Solar photovoltaic
WES	Wind energy systems
BESS	Battery energy storage system
EVs	Electric vehicles
U-SWBEV	UPQC with RES, EV and Battery
ANFIS	Artificial neuro-fuzzy interface system
ANN	Artificial neural network
FL	Fuzzy logic
FACTS	Flexible Alternating Current Transmission Systems
UPFC	Unified Power Flow Controller
THD	Total Harmonic Distortion
SVC	Static Var Compensator
SOC	Short circuit current
DVR	Dynamic Voltage Restorer
DSTATCOM	Distribution Static Synchronous Compensator
OCV	Open circuit voltage
SHAPF	Shunt active power filters
VSC	Voltage Source Converters
GA	Genetic Algorithm
PSO	Particle swarm optimization
ACO	Ant colony optimization
COV	Cut of voltage
NOV	Nominal Voltage
DLCV	DC Link Voltage
SOC	State of charge of battery
MSF	Membership Function
ST	Station
PLL	Phase-Locked Loop
PWM	Pulse Width Modulation
PSF	Performance score function
MVP	Most Valuable Player
FP	Franchise player
P&O	Perturb and observe method
MPPT	Maximum power point tracking technique
LPF	Low pass filter
FF	Fitness function
MNI	Maximum number of iterations
V_{S_abc}	Source voltage inphase
i_{S_abc}	Source current inphase
i_{sh_abc}	Shunt filter supplied in phases
V_{l_abc}	Load voltage in phases
V_{se_abc}	Series injected voltage in phase
$V^{ref}_{se\_dq}$	Series filter reference voltage in dq
$i^{ref}_{sh\_abc}$	Reference injected SHAPF current in phases
i_{l_abc}	Load current in phases
R_{sh}	Shunt filter resistance
R_{se}	Series filter resistance
L_{sh}	Shunt filter inductance
L_{se}	Series filter inductance
C_{dc}	DC link capacitor
V_{dc}	Voltage across DC link capacitor
i_{ph}	Photo source current
i_d	Diode Forward conducting current
$R_{s,PV}$ **and** $R_{sh,PV}$	Series and parallel resistances of cell
$i_{sh,PV}$	Parallel current of PV cell
i_{PV}	PV cell output current
$i_{PV,m}$, $V_{PV,m}$	Module current and voltage
$i_{s,PV}$	Reverse saturation current
i_{rs}	Reverse saturation current
V_{oc}	Open circuit voltage
N_s	Number of series connected PV cell
N_p	Number of parallel connected PV cell
G	Solar irradiance (W/m^2)
T	Variation in PV cell temperature
P_{PV}	Output PV power
P_{BS}	Battery output power
η	Diode ideal factor
k	Boltzmann's constant
i_{mo}	Module current
Q	Battery's capacity
R	Internal resistance of battery
i_{BESS}	Battery current
V_{BESS}	Battery voltage
P_{BESS}	Battery power
ω	Rotor's rotational velocity
K	Polarization value

V_w	Wind speed
P_w	Wind power
P_L	Load power
P_{EV}	EV power
R_b	Blade's radius
R_{st}	Tip speed ratio
ρ	Air density
T_{mop}	Torque output
P_{mop}	Mechanical power output
C_p	Coefficient of power
Nr	Speed ratio
θ_p	Blade's pitch angle
V_{dc}^{ref}	Reference value of DLCV
K_p, K_i, K_d	Gain values of PIDC
Δi_{dc}	Error current of SHAPF
$i_{l\_d} i_{l\_q}$	Load current in dq
$V_{s\_d}^{ref} V_{s\_q}^{ref}$	Reference source current in dq
$V_{l\_abc}^{ref}$	Reference load voltage in phase
$V_{s\_d} V_{s\_q}$	Source voltage in dq
I_n	Individual harmonic current distortion
I_1	Fundamental harmonic current distortion
I_2	2nd harmonic current distortion
γ	Euclidean distance